NASA Contractor Report 174829

Behavior of Turbulent Gas Jets in an Axisymmetric Confinement

Ronald M. C. So and Saad A. Ahmed

Arizona State University
Tempe, Arizona

January 1985

Prepared for

NATIONAL AERONAUTICS AND SPACE ADMINISTRATION
Lewis Research Center
Under Grant NAG 3-260

Table of Contents

Table of Contents (Cont'd)

Notation

English Letters

a, b, b_1	constants defined in eqs. (1) and (2)
C	constant defined in eq. (4)
D	diameter of tube or jet nozzle
k	turbulent kinetic energy
$K(x)$	velocity profile shape parameter defined in eq. (3)
M	momentum flux
M_r	momentum flux of air jet at $U_j = 66.8$ m/s
r	radial coordinate
$r_{1/2}(x)$	jet half-width
$Re_j = U_j D_j/\nu$	jet Reynolds number
Re_t	turbulent Reynolds number defined in eq. (12)
u	instantaneous or fluctuating axial velocity
u'	rms of u
U	mean axial velocity
V	mean radial velocity
w	instantaneous or fluctuating circumferential velocity
w'	rms of w
x	axial coordinate

Greek Letters

$\eta = r/x$	normalized r coordinate
$\xi = r/r_{1/2}$	normalized r coordinate
ν	kinematic viscosity of fluid
ν_T	turbulent kinematic viscosity

ρ	density

Subscripts

a	air or ambient condition
e	external stream of coaxial jets
j	jet
m	mixture
o	centre line
x	any x location

Abstract

The understanding of the mixing of confined turbulent jets of different densities with air is of great importance to many industrial applications, such as gas turbine and ramjet combustors. Although there have been numerous studies on the characteristics of free gas jets, little is known of the behavior of gas jets in a confinement. The present investigation addresses this question directly and reports on the fluid dynamics of confined turbulent gas jets.

The jet, with a diameter of 8.73 mm, is aligned concentrically with a tube of 125 mm diameter, thus giving a confinement ratio of ~205. The arrangement forms part of the test section of an open-jet wind tunnel. Experiments are carried out with carbon dioxide, air and helium/air jets at different jet velocities. Mean velocity and turbulence measurements are made with a one-color, one-component laser doppler velocimeter operating in the forward scatter mode.

Measurements show that the jets are highly dissipative. Consequently, equilibrium jet characteristics similar to those found in free air jets are observed in the first two diameters downstream of the jet. These results are independent of the fluid densities and velocities. Decay of the jet, on the other hand, is a function of both the jet fluid density and momentum. In all the cases studied, the jet is found to be completely dissipated in ~30 jet diameters, thus giving rise to a uniform flow with a very high but constant turbulence field across the confinement.

1. Introduction

1.1 Motivation

Isothermal turbulent jet mixing in a confined swirling flow has been recently investigated by So et al. (1984). Their objectives are to study the effects of swirl and density difference on confined jet mixing and their results are reported by So et al. (1985) and Ahmed et al. (1985). In order to achieve these objectives they have also examined the behavior of confined swirling flow and confined jet flow in the same test facility. Their preliminary results on confined gas jets show that the jet flow is highly dissipative. However, they have not studied the phenomenon in detail, especially the effects of density difference. The present investigation is a continuation of their effort and is carried out in the same test facility (So et al. 1984). In order to better understand the phenomenon, confined jets of helium, air and carbon dioxide are investigated so that the effects of density difference can be examined in more detail.

1.2 Review of Related Work

Confined jets have not been extensively investigated in the past. This is especially true of jets of different densities issuing into a confinement of stationary air. Among the recent work on confined jets are the study of Abramovich et al. (1969) and the experiment of Janjua et al. (1983). In the experiments of Abramovich et al. (1969), jets of heated air, helium and Freon-12 were investigated. The area ratio of the confinement to the jet was 9. Several velocity ratios (external flow to jet flow) were studied and these ranged from 0 to 3. A major portion of their study was on coaxial jets, only one case was on confined jets. It was not clear from their paper (Abramovich et al. 1969) whether the cylindrical confinement formed part of

a wind tunnel or terminated after a finite length. Since the two situations gave different end conditions, a comparison of their data with those of So et al. (1984) and Janjua et al. (1983) has to be carried out with caution. Also, their jet fluid temperatures varied from 20 to 300°C. Consequently, non-isothermal mixing resulted and thermal buoyancy effects were also present in the flow field. Their results showed that a potential core existed for confined gas jets, an observation not found in the experiments of So et al. (1984) and Janjua et al. (1983). This potential core was found to decrease with decreasing jet fluid density. The jet persisted for a substantial distance downstream, $x/D_j > 30$. Besides, self-preserving velocity profiles were measured for different density gases, ranging from lighter to heavier than air jet fluids. On the other hand, the experiment of Janjua et al. (1983) was carried out with air only and in a confinement four times larger than the jet cross-sectional area. Their measurements showed that the jet-like behavior vanished after about 10 jet diameters downstream, and no recirculation region was measured behind the sudden expansion. Consequently, the flow was neither jet-like nor completely resembled that through a tube expansion (Eaton and Johnston 1980). Besides, the high jet turbulence was found to decrease rapidly in about the same distance. This behavior resembled the highly dissipative jet characteristics observed by So et al. (1984) and was in stark contrast to the measurements of Abramovich et al. (1969).

Coaxial jet mixing of dissimilar gases was also investigated by Alpinieri (1964) and Zakkay et al. (1964). In the experiments of Alpinieri (1964), a slightly heated jet of hydrogen or carbon dioxide was issued into a co-flowing air stream. The area ratio of the tube to the jet was 16 and the velocity ratio investigated ranged from .5 to 1.25. Therefore, the

conditions were quite similar to those studied by Abramovich et al. (1969). On the other hand, the helium, hydrogen and argon jet into air experiments of Zakkay et al. (1964) were carried out in a tube whose area was 12 times larger than the jet and the air stream was supersonic, with a Mach number of 1.6. In spite of the different conditions, the coaxial jet experiments revealed the following results. Mass was found to diffuse more rapidly than momentum. The potential core of the inner jet was directly related to $(\rho_j U_j / \rho_e U_e)^{1/2}$. Centerline decay of mass concentration was found to be proportional to $(x/D_j)^{-2}$, but the centerline decay of velocity was not. Finally, segregation of the streams was not observed when either the velocities or the mass flows of the streams were equal.

Turbulent free jet experiments with different density gases have been studied by numerous investigators. Among these are the air jet studies of Becker et al. (1967), Wygnanski and Fiedler (1969) and Maestrello and McDaid (1971), the helium jet experiment of Way and Libby (1971), the CH_4 jet of Birch et al. (1978) and the gas jet experiments of Keagy and Weller (1949) and Sforza and Mons (1978). The general findings of these studies were power-law decay for both centerline velocity and concentration, even though widely different values were reported for the exponent (Schetz 1980). The influence of density on centerline decay of velocity and concentration was very strong. Also, the mass-momentum transfer ratio across the jet was found to be varying rather than constant. Indeed, the measured turbulent Schmidt number varied from ~ .7 in the jet core to ~ 1.2 towards the jet boundary. Concentration fluctuations were also measured by Way and Libby (1971), Becker et al. (1967) and Birch et al. (1978). Hot-wire technique was used by Way and Libby (1971) while Becker et al. (1967) and Birch et al. (1978) made use of optical techniques. The measurements of Birch et al.

(1978) revealed consistent deviation from Gaussian statistics of the concentration fluctuations along the centerline of the jet.

1.3 Present Objectives

From this brief review, it can be seen that not much is known about the behavior of gas jets in a confinement. The few measurements available (Abramovich et al. 1969; Janjua et al. 1983; So et al. 1984) show conflicting behavior for the confined jets. While the more recent work reveals the jet to be highly dissipative, the earlier study of Abramovich et al. (1969) shows that the jet flow is quite regular. The difference in behavior could be due to different end conditions in the test facility. However, the observed conflicting behavior arouses curiosity, thus the need to investigate confined gas jets systematically. In view of this and a general lack of knowledge of this interesting problem, confined gas jets are investigated in detail in the present study.

2. The Experimental Program

2.1 Experimental Set-up

The present series of experiments is carried out in the same facility used by So et al. (1984). In that facility, the jet nozzle with a diameter of 8.73 mm, is mounted concentrically within a vane swirler located in a circular tube of diameter 125 mm. This gives an area ratio of ~ 205. The tube, of length 4.0 m, forms part of the test section in an open-jet wind tunnel. For confined jet studies, the blower in the wind tunnel is turned off. Separate gas supply is being delivered to the jet nozzle via a heat exchanger. With this arrangement, an axisymmetric, isothermal confined jet is created for detailed investigation. A schematic of the test facility is shown in Figure 1.

A one-color, one component LDA system operating in the forward scatter mode is used to measure axial and circumferential velocities, u and w, respectively (Figure 2). The technique and data reduction procedure worked out by So et al. (1984) are used in the present experiment, except that 3-9 blocks of 1024 samples are used to determine the velocity statistics. A block diagram of the LDA and data acquisition equipment is shown in Figure 2. Three different gases, namely, helium/air mixture, air and carbon dioxide, are used as jet fluids. This provides a density ratio range of .23 $\leq \rho_j/\rho_a \leq 1.52$. Temperatures of the jet fluids and the surrounding air are maintained to within $\pm 1^{\circ}F$ of each other by passing the gas through a heat exchanger before delivering to the jet nozzle. This way, true isothermal, inhomogeneous mixing is achieved. Further details of the facility and diagnostic techniques can be found in So et al. (1984).

So et al. (1984) have carried out experiments to investigate the effects of seeding on the mixing behavior in the case of air jets in

confined swirling flow. They found that repeatable and reliable measurements could be obtained by seeding the external flow in the plane of measurement only. It was not necessary to seed the jet. Therefore, the jet conditions were not compromised by the necessity of seeding. Before carrying out the present series of experiments, the effect of seeding on jet mixing is also examined. The experiment is carried out with an air jet set at U_j = 23.4 m/s. In one case, seeding is provided to the jet only, while in the second case, seeding is provided at the plane of measurement upstream of the jet and none to the jet at all. Measurements at x/D_j = 1.5 and 10 reveal that there are no discernible differences between the two sets of data. Seeding the external air only is also found to be applicable for carbon dioxide jets. However, it fails to give accurate and repeatable results for pure helium jets. The reason is not enough seeding can penetrate into the jet mixing region to give a decent LDA signal for processing. Consequently, the helium jet has to be seeded directly, and this results in a jet of helium/air mixture. A minimum amount of seeding is provided to the helium jet so that the resultant mixture density is still small compared to that of air. The mixture density is determined by measuring the composition of the helium/air mixture and assuming the helium and air to be homogeneously mixed inside the jet nozzle.

Since the present facility and LDA arrangement cannot be used to measure the flow at $x/D_j < 1$, the jet exit velocity is measured by two alternative methods. In one case, a pitot tube is positioned at the center of the jet exit plane, while in the second method, a rotor-meter is used to measure the gas volume flow through the jet nozzle. Both methods give jet exit velocity, U_j, accurate to $\pm 3\%$ of each other.

2.2 Test Conditions and Results

Altogether seven sets of experiments are carried out, two sets each for helium/air mixture and carbon dioxide and three sets for air. The jet velocities are selected so that for all jet fluids investigated, jets of equal exit velocity and momentum flux but different fluid density are examined. A summary of the test conditions is given in Table 1. Although the helium/air jet Reynolds numbers are very low, the jets are made fully turbulent by designing the nozzle with a sudden expansion (So et al. 1984) in accordance with the studies of Eaton and Johnston (1980). Consequently, all jets tested are fully turbulent and Reynolds number effects are not important. The only parameters of importance in the experiments are ρ_j/ρ_a, U_j and $\dot{M}_j/\dot{M}_r$.

Since the preliminary results of So et al. (1984) show that the jets are highly dissipative, it is anticipated that axial pressure gradient set up by the jet flow in the tube will not be an important parameter in the flow. In spite of this, wall static pressure drop is measured in addition to axial and circumferential velocities at selected x/D_j locations. Velocity measurements are carried out from $x/D_j \geq 1$ to whatever x/D_j location downstream where the jet ceases to exist.

The fluid dynamic properties reported in this study include both the mean flow behavior and the turbulent normal fluxes. These are limited to measurements in the axial and circumferential directions only. Radial measurements are not made and therefore are not reported. Concentration distributions and other flux measurements have been reported by Ahmed and So (1984). The velocity measurements are Tabulated in Tables 2-11. Centerline measurements of carbon dioxide, air and helium/air jets are listed in Tables 2, 3 and 4, respectively. Velocity profile data are listed in Tables 5 and

6 for carbon dioxide jets, in Tables 7, 8 and 9 for air jets and in Tables 10 and 11 for helium/air jets.

3. Discussion of Results

The present study is a continuation of an investigation on isothermal mixing in an axisymmetric combustor. It seeks to answer the question raised by So et al. (1984) on the behavior of confined gas jets. The preliminary results of these investigations reveal that such jets are highly dissipative. Consequently, the resultant flow inside the confinement neither resembles that of a free jet flow with favorable pressure gradient nor that of a flow through a sudden expansion. The first and foremost objective of this study, then, is to investigate the fluid dynamics of confined gas jets in detail. Through this, it is hoped that the behavior of confined gas jets can be better understood.

Wall static pressure measurements are made for all jet conditions listed in Table 1. Since the wall static pressure to be measured is very small, the resulting scatter in the data is very large. The scatter improves as U_j increases. In spite of this, the measurements reveal that the wall static pressure distribution for the first 100 D_j is essentially similar for all jets tested. However, because of the scatter, it is not possible to conclude that the wall static pressure is constant over the region $x/D_j \leq 100$. As later analysis of the jet behavior will demonstrate, the normalized jet characteristics are typical of free jets with zero streamwise pressure gradient effects. Therefore, it can be concluded that axial pressure gradient is not an important parameter in the confined jets studied.

Contrary to free jet results (see e.g., Wygnanski and Fiedler 1969; Maestrello and McDaid 1971; Birch et al. 1978) and the confined jet measurements of Abramovich et al. (1969), the existence of a potential core immediately downstream of the jet exit is not observed. Instead, the jet

centerline axial velocity, U_o, is found to decrease to .33 - .48 U_j, even at $x/D_j \simeq 1.3$ (Figure 3). These measurements are quite suspicious and prompt a continuity check on the measured axial velocity profiles, U(r), at $x/D_j \leq 2$. Since the density profiles of the helium/air and carbon dioxide jets are not known, the check is carried out with the measured air jet profiles only. Mass flow rates obtained by integrating U(r) at $x/D_j \leq 2$ (Figures 7-9) give values that agree to within 8% of those calculated from $D_j = 8.73$ mm and U_j listed in Table 1 for the air jets. In view of this, the measured U_o shown in Figure 3 can be considered to be essentially correct for all confined jets studied.

3.1 Centerline decay of gas jets.

The jet centerline velocity decays quickly for all confined jets examined. However, the decay rate is different for different jets (Figure 3). Two distinct decay curves can be identified, one for helium/air and air jets at $U_j \leq 66.8$ m/s, another for air jet at $U_j = 152.8$ m/s and CO_2 jets. Among the two, the slower decaying one is that for CO_2 jets and air jet at $U_j = 152.8$ m/s. All confined jets decay much faster than free jets of air, helium, CH_4 and CO_2 shown in Figure 3 for comparison. While ρ_j/ρ_a controls the jet decay rate in the case of free jets, such is not necessarily the case in the confined jets studied. It seems that $\dot{M}_j/\dot{M}_r$ is also an important parameter. For $\rho_j/\rho_a \leq 1$, the decay rate is essentially controlled by $\dot{M}_j/\dot{M}_r$. The results seem to show that the jet decays faster when $\dot{M}_j/\dot{M}_r \leq 1$. Although the $\dot{M}_r$ selected is arbitrary, it serves to show that there is a critical $\dot{M}_r$ that governs the decay of gas jets with $\rho_j/\rho_a \leq 1$. For the present series of experiments, $\dot{M}_r = .027$ kgmf. The actual $\dot{M}_r$ may be between

.027 kgmf and .141 kgmf, the last value being the $\dot{M}_j$ of the air jet at U_j = 152.8 m/s. The density ratio, ρ_j/ρ_a, as long as it is greater than 1, seems to have a great effect on the jet decay. A slightly heavier jet ($\rho_j/\rho_a \geq 1.52$) with $\dot{M}_j/\dot{M}_r \leq 1$ is enough to decrease the jet decay to about that of a jet with $\rho_j/\rho_a \leq 1$ and $\dot{M}_j/\dot{M}_r = 5.23$.

The extremely fast decay of confined jets is indicative of the highly dissipative nature of such flows. By way of explanation, the following conjecture can be considered. Stationary fluid inside the tube is being pushed by the incoming jet fluid. Because of the confinement and the large amount of fluid to be pushed by the jet, the resistance encountered by the jet is very large. Consequently, the jet has to do work on the body of stationary fluid and its momentum is quickly dissipated. The body of fluid is set into motion by the action of the jet and at some distance downstream, the fluid in the tube would achieve a velocity equal to U_j/area ratio (for $\rho_j/\rho_a = 1$ case only). More will be said about the dissipative phenomenon later.

If this line of reasoning is followed, then it will be possible to explain the slower decay of the CO_2 jets with $\dot{M}_j/\dot{M}_r < 1$. When the jet issues into the confinement, it impinges normally on the column of stationary air. Part of the jet fluid will be deflected radially outward, thus giving rise to a significant radial velocity. This could be one of the reasons why a potential core is not observed in the jet and why the centerline jet velocity decreases so rapidly. The phenomenon is analogous to a jet impinging normal to a solid surface. In this case, the jet centerline velocity is reduced to zero at the surface and the jet axial momentum minus frictional losses is completely converted to radial momentum.

In the case of the confined jet, the measurements seem to indicate that the stationary air column offers sufficient resistance to the incoming jet to bring its axial velocity down rapidly. Part of the jet axial momentum will be expanded to do work against the air column, part to overcome frictional losses and part is converted to radial momentum. This conjecture could be substantiated by measuring the radial velocity. If the results show a radial velocity significantly larger than that measured in a free jet, the above explanation offered for the rapid decay of the confined jet is essentially correct. Assuming this conjecture to be plausible for the moment, the slower decay of the CO_2 jets follows directly from this line of reasoning. Since the density of CO_2 is heavier than that of air and helium, it will take longer for the CO_2 particle to diffuse outward by the same radial distance. Hence, the slowed decay of the CO_2 jets. In other words, buoyancy also plays a part in the decay of confined jets.

The shape of the decay curves suggests that U_o decays exponentially rather than in a power-law manner as indicated by the measurements of Abramovich et al. (1969). A semi-logarithmic plot of U_j/U_o versus x/D_j is shown in Figure 4. Indeed, to within experimental measurement errors, the decay curves of Figure 3 become linear curves in Figure 4. The difference in decay rate of the CO_2 jets and the air jet at U_j = 152.8 m/s is made more evident, and the plot reveals that the air jet at U_j = 152.8 m/s is the slowest decaying confined jet examined. For comparison purposes, the confined heated air jet (ρ_j/ρ_a = .59) data of Abramovich et al. (1969) is also included in Figure 4. The exponential decay behavior of the present confined jets is clearly evident. However, the measurements of Abramovich et al. (1969) do not seem to fall in line with the present results. Even though ρ_j/ρ_a = .59 and $10 \leq U_j \leq 50$ m/s for the heated air jet, its decay is

slowest compared to the other isothermal jets. This seems to show that thermal buoyancy effects could play an important role in confined jet decay. It is interesting to note that the decay slope of the CC_2 jets is about $(\rho_j/\rho_a)^{-3/2}$ times the decay slope of the helium/air and air jets. This means that for confined gas jets with $\dot{M}_j/\dot{M}_r \leq 1$, the decay curves can be described by

$$\ell n \frac{U_j}{U_o} = a\left(\frac{x}{D_j}\right) + b; \qquad \frac{\rho_j}{\rho_a} \leq 1, \tag{1}$$

$$\ell n \frac{U_j}{U_o} = \left[\frac{\rho_j}{\rho_a}\right]^{-3/2} a\left(\frac{x}{D_j}\right) + b_1; \qquad \frac{\rho_j}{\rho_a} > 1, \tag{2}$$

where present results give $a = .23$, $b = .52$ and $b_1 = .66$. Equations (1) and (2) are independent of U_j as long as $\dot{M}_j/\dot{M}_r \leq 1$.

The slower decay of the high velocity air jet can now be explained as follows. If the above conjecture is plausible, then the work required to push the stationary air column is fixed for a given confinement geometry. The amount of radial momentum derivable from the jet momentum will also have to be geometry dependent. Therefore, once the geometry is fixed, this, too, cannot vary significantly. For a high velocity jet, there is more momentum available and this allows the jet to penetrate further into the confinement before decaying. Hence, the slower rate observed for the $U_j = 152.8$ m/s air jet. The present measurements suggest that there is a critical jet momentum value above which the jet decays slower for $\rho_j/\rho_a = 1$ jets.

Evidence of the highly dissipative nature of the confined jets can also be found by examining the behavior of u'_o and w'_o; the rms values of the centerline turbulent normal stress in the axial and circumferential directions, respectively (Figures 5 and 6). For free jets, u'_o/U_o increases

with x/D_j in the initial region of the jet, then becomes constant in the equilibrium region far downstream. The constant value reached by air jet is ~ .35 (Wygnanski and Fiedler 1969). Figure 5 shows that $u_o'/U_o \simeq .35$ in the region $x/D_j \leq 5$ for all confined jets studied. Thereafter, u_o'/U_o increases with x/D_j. The rate of increase is greatest for jets with $\dot{M}_j/\dot{M}_r \leq 1$ and $\rho_j/\rho_a \leq 1$, and slowest for jets with $\dot{M}_j/\dot{M}_r > 1$ and $\rho_j/\rho_a = 1$.

The high level of turbulence measured at the jet centerline lends credence to the above conjecture for the confined jet behavior. Also, the higher rate of increase of u_o'/U_o and w_o'/U_o with x/D_j for air and helium jets with $\dot{M}_j/\dot{M}_r \leq 1$ compared to CO_2 jets supports the argument that the initial behavior of the confined jet is quite similar to that found in jet impinging normal to a solid surface. If the turbulence field is assumed to be isotropic, then $v_o' \simeq w_o'$ and this suggests that the radial velocity in the initial region of the jet is possibly quite large, too. This, again, lends credence to the impinging jet analogy.

It seems that dissipation is responsible for bringing the jet into an equilibrium state within a short distance downstream. Another indication of the equilibrium nature of the flow can be found by comparing the value $\bar{k}_o/U_o$ with the equilibrium measurements of Wygnanski and Fiedler (1969) in a free jet. The present results give $\bar{k}_o/U_o \simeq .29$ in the region $x/D_j \leq 5$ if $w_o' = v_o'$ is assumed. This compares well with a value of .31 measured by Wygnanski and Fiedler (1969). The turbulence field is not as isotropic as that observed in free air jets. The ratio u_o'/w_o' is ~ 1.8, compared to a value of ~ 1.2 measured in free jets. However this ratio, u_o'/w_o', remains fairly constant over the range $x/D_j \leq 20$, an indication that the jets are in a continued state of equilibrium through this distance. The subsequent

increase of u_o'/U_o and w_o'/U_o (Figures 5 and 6) is a consequence of the rapid decay of the jet and is not due to an increase in the turbulence intensities of the flow. More will be said about this later when the turbulence profiles are examined.

3.2 Mean velocity profiles.

The mean axial velocity profiles, U(r), normalized by $U_o(x)$ are plotted versus r. Profiles for the air jets are shown in Figures 7-9, for the CO_2 jets in Figures 10-11 and for the helium/air jets in Figure 12. The symmetry of the jets is checked by measuring U(r) on both sides of the tube centerline. This is carried out at selected x/D_j locations. For those locations with such measurements, the data in Figures 7-12 are shown with open and filled symbols. In general, the confined jets can be considered to be quite symmetric about the tube centerline. There is some scatter in the data. However, it is not excessive in the jet near field. The scatter becomes progressively worse as the measurement moves downstream. Reason is the low mean flow in a background of very high turbulence. As for the scatter in the jet near field, it is due to the relatively large measuring volume of the beam crossing (.99 mm x .12 mm) and the steep gradient of the velocity profiles. On the other hand, the excessive scatter seen in the helium/air jet measurements (Figure 12) is probably also due to insufficient data block used to evaluate the velocity statistics (3-6 blocks compared to 6-9 blocks for air and CO_2 jets). In spite of this, the trend of the data is clearly evident and is in general agreement with those found in air and CO_2 jets.

The flow is clearly jet-like, at least for the first 14 diameters downstream of the jet exit. There is a small reverse flow region which extends from $2 < x/D_j < 14$ in the region near the tube wall. The largest

extent of this reverse flow region is found in the case of the air jet with U_j = 152.8 m/s. Even then, the reattachment length is less than 5 step height. For the other cases, the reattachment length is less than 3 step height. According to Eaton and Johnston (1980), the reattachment length for sudden expansion flow should be around 6-10 step heights. This together with the fact that the U(r) profiles (Figures 7-12) do not resemble those found in sudden expansion flows (Eaton and Johnston 1980) indicates that the flow inside the tube is actually a jet-type flow. More will be said about this point when the turbulence profiles are analyzed.

According to Keagy and Weller (1949), free gas jet profiles in the equilibrium region can be described by the expression,

$$\frac{U}{U_o} = e^{-K\eta^2}, \tag{3}$$

where K takes on different values for different gases. If the confined jets are being forced into an equilibrium state by the highly dissipative phenomenon, then the measured U/U_o can be appropriately described by (3). This is indeed the case, as shown by the good correlation between measurements and the solid and dashed curves plotted in Figures 7-12. The solid and dashed curves are derived from (3) with different K values. A list of the K values and the jet half-width $r_{1/2}$, thus determined is given in Table 12. For most cases, the flow is seen to be jet-like up to $x/D_j \leq 14$.

Contrary to the findings of Keagy and Weller (1949), K is found to be a function not of gas density but of x and $\dot{M}_j/\dot{M}_r$. The fullness of the U(r) profiles is measured by the value of K. For free jets, K = 57 for helium, 88 for nitrogen and 101 for carbon dioxide (Keagy and Weller 1949).

Therefore, helium jets spread faster than nitrogen jets, which in turn spread faster than carbon dioxide jets. For confined gas jets, the spread of the jets is more a function of $\dot{M}_j$ than ρ_j. Also, the jet shows a trend of ''narrowing'' as it moves downstream which indicates that the jet is dissipated in a confinement. The disappearance of the jet in a confinement is not surprising. What is surprising is that it occurs in such a short distance and seems to be only controlled by the jet momentum, $\dot{M}_j$. This evidence further substantiates the claim that the present confined jets are highly dissipative.

The local equilibrium nature of the jets suggest that all U/U_o profiles can be described by one similarity expression, such as,

$$\frac{U}{U_o} = e^{-c\xi^2}, \tag{4}$$

where $\xi = r/fn(x)$ and c is a true constant. An examination of Table 12 reveals that $Kr^2_{1/2}/x^2$ is a constant and can be approximated by $\ell n\ 2$. Therefore, this indicates that $\xi = r/r_{1/2}(x)$, $c = \ell n\ 2$ and all measured jet profiles can be described by

$$\frac{U}{U_o} = e^{-\xi^2 \ell n\ 2}. \tag{5}$$

This profile also describes the free jet measurements of Keagy and Weller (1949), because their data show that $K\eta^2_{1/2} = \ell n\ 2$, where $\eta_{1/2} = r_{1/2}/x$. On the other hand, Abramovich et al. (1969) found that their data was best correlated by an expression,

$$\frac{U}{U_o} = \frac{1}{2}\left(1 + \cos\frac{\pi}{2}\xi\right), \tag{6}$$

even though (5) can be used to adequately describe their results. Again, the expression is valid for all jet fluid densities and velocities. It is also valid for non-zero external stream if U and U_o are taken to be the excess velocities over that of the external stream. All these suggest that the flow is jet-like, and that axial pressure gradient effects are not important.

Further evidence that the flow is in local equilibrium and free of streamwise pressure gradient effects can be found by examining the high Reynolds number, compressible, axisymmetric thin shear layer equations for zero pressure gradient flow. The equations are:

$$\frac{\partial \rho r U}{\partial x} + \frac{\partial \rho r V}{\partial r} = 0 \ , \tag{7}$$

$$\rho r U \frac{\partial U}{\partial x} + \rho r V \frac{\partial U}{\partial r} = \frac{\partial}{\partial r}\left(r \mu_m \frac{\partial U}{\partial r}\right) , \tag{8}$$

$$\rho r U \frac{\partial \Theta}{\partial x} + \rho r V \frac{\partial \Theta}{\partial r} = \frac{\partial}{\partial r}\left(r \mu_s \frac{\partial \Theta}{\partial r} \right), \tag{9}$$

where V is the mean radial velocity, ρ is the mean mixture density, Θ is the mass fraction of jet fluid, $\mu_m(x,r)$ is the turbulent viscosity for momentum transport and $\mu_s(x,r)$ is the corresponding quantity for mass transport. In writing down (7)-(9), the turbulent fluxes $-\rho\overline{u'v'}$, and $-\rho\overline{v'\Theta'}$ have been replaced by $\mu_m(\partial U/\partial r)$ and $\mu_s(\partial \Theta/\partial r)$, respectively. Also, molecular diffusion has been neglected compared to turbulent diffusion. The relation between ρ and Θ for binary gas mixing is given by

$$\frac{1}{\rho} = \frac{1}{\rho_a} - \left(\frac{1}{\rho_a} - \frac{1}{\rho_j}\right)\Theta \ , \tag{10}$$

Boundary conditions for (7)-(10) are:

$$U(x,o) = U_o(x) \ , \tag{11a}$$

$$V(x,o) = 0 \ , \tag{11b}$$

$$\theta(x,o) = \theta_o(x) \ , \tag{11c}$$

$$\rho(x,o) = \rho_a + \rho_o(x) \ , \tag{11d}$$

$$U(x,\infty) = \theta(x,\infty) = 0 \ , \tag{12a}$$

$$\rho(x,\infty) = \rho_a \ , \tag{12b}$$

where $U_o(x)$, $\theta_o(x)$ and $\rho_o(x)$ are unknowns to be determined.

A closed form solution to (7) - (10) subject to boundary conditions (11) - (12) and based on the parameter $\xi = r/r_{1/2}(x)$, where $r_{1/2}(x)$ is an unknown to be determined, has been obtained by Jo and Liu (1985). The results are:

$$\frac{U}{U_o} = e^{-\xi^2 \ell n\ 2} \ , \tag{13}$$

$$\frac{\theta}{\theta_o} = \left[\frac{1 + (\sigma_1 - 1)\ \bar{P}}{1 + (\sigma_1 - 1)\ \bar{P}\ e^{-c_1\xi^2}}\right] e^{-c_1\xi^2} \ , \tag{14}$$

$$\frac{\rho - \rho_a}{\rho_o} = e^{-c_1\xi^2} \ , \tag{15}$$

$$\mu_m(x,\xi) = \frac{(\rho_a + \rho_o)\ U_o\ r_{1/2}}{Re_t}\left[\frac{H(x,\xi)}{\xi^2}\right] \ , \tag{16}$$

$$\mu_s(x,\xi) = \frac{(\rho_a + \rho_o)\ U_o\ r_{1/2}}{Re_t}\left[\frac{H_1(x,\xi)}{\xi^2}\right] \ , \tag{17}$$

$$H = 1 - \frac{c\,(\sigma_1 - 1)\,\bar{P}}{b + 2c(\sigma_1 - 1)\,\bar{P}}\, e^{-a\xi^2}$$

$$- \frac{b + c\,(\sigma_1 - 1)\,\bar{P}}{b + 2c\,(\sigma_1 - 1)\,\bar{P}}\, e^{-c\xi^2}, \tag{18}$$

$$H_1 = \frac{c}{c_1}\left(1 - e^{-c\xi^2}\right)\left[1 + (\sigma_1 - 1)\,\bar{P}\, e^{-c_1\xi^2}\right], \tag{19}$$

where $\bar{P} = \rho_o/(\rho_j - \rho_a)$, $\sigma_1 = \rho_j/\rho_a$, $c = \ell n\ 2$, $a = c + c_1$ and $b = a + c$. There are two free parameters in these solutions and these are c_1 and Re_t, where Re_t can be interpreted as the turbulent Reynolds number. The parameters are constant for a given jet fluid. However, they can vary from one jet fluid to another. The variations of U_o, θ_o, ρ_o and $r_{1/2}$ with x are given by

$$\frac{U_o}{U_j} = \frac{Q\,\bar{P}}{b + 2c\,(\sigma_1 - 1)\,\bar{P}}, \tag{20}$$

$$\theta_o = \frac{\sigma_1\,\bar{P}}{1 + (\sigma_1 - 1)\,\bar{P}}, \tag{21}$$

$$\frac{r_{1/2}}{(r_{1/2})_j} = \frac{[b + 2c\,(\sigma_1 - 1)\,\bar{P}]^{1/2}}{Q^{1/2}\,\bar{P}}, \tag{22}$$

$$\frac{d\bar{P}}{dZ} = -\frac{Q^{1/2}[1 + (\sigma_1 - 1)\,\bar{P}]\,\bar{P}^{2}}{[b + 2c\,(\sigma_1 - 1)\,\bar{P}]^{1/2}}, \tag{23}$$

where $Q = b + 2c\,(\sigma_1 - 1)$, $Z = 4c^2x/(r_{1/2})_j\,Re_t$ and $(r_{1/2})_j$ is $r_{1/2}$ at the jet unit. These results compare well with free gas jet measurements (So and Liu 1985) and predict the measured linear decay of U_o and ρ_o correctly.

The results show that $r_{1/2}$ is a linearly increasing function of x, a fact amply demonstrated by Figure 13, and $U_o \propto x^{-n}$, where n is a function of σ_1. This last result seems to be in conflict with the exponential decay shown in Figure 4. However, a replot of the data in Figure 14 reveals that a power-law decay for U_o is also appropriate. As before, n is dependent on the ratio ρ_j/ρ_a only when this is larger than one. Figure 14 shows that n for Freon-12 jets ($\rho_j/\rho_a = 3.7$) is larger than that for CO_2 jets, which in turn is larger than helium air and air jets. The fact that the measured velocity profiles agree with the solution of (7)-(10) confirms that the flow is jet-like, free of pressure gradient effects and is in a self-preserving state, at least locally.

If the jet is highly dissipative, then the jet momentum is not conserved. The following calculations are performed to estimate the momentum loss by the jet in the process of penetrating through the confinement. Only the air jet experiments are considered because the density profiles of the other two gas jets are not known. The momentum flux across the tube at any x location is estimated by integrating the measured U profile across the tube. This is compared with the corresponding value obtained by integrating (3) across the jet. The result gives the jet momentum flux to be about 98% of that through the tube at $x/D_j \leq 2$. Therefore, the momentum flux at these locations is essentially all concentrated in the jet. The calculations, $\dot{M}_x/\dot{M}_j$, where $\dot{M}_x$ is the jet momentum flux at any x, for the three air jets are plotted versus x/D_j in Figure 15. It can be seen that the jets lose more than 60% of their axial momentum in just one jet diameter downstream. As discussed before, not all

of this momentum is lost. Part of the axial momentum is converted to radial momentum, part of it goes into promoting turbulence, as reflected by the rather high turbulence level measured in the initial region of the jets, and part of the momentum is expanded to do work in the column of stationary air. The present measurements do not provide sufficient information to allow the exact amount for each category to be calculated. Therefore, it is not possible to evaluate the actual momentum loss by the jets. To do this, the radial velocity and the turbulent shear fluxes need to be measured.

3.3 Turbulence distributions.

The turbulence profiles of u' and w' are again normalized with U_o. They are shown in Figures 16-24. The measurements of u' are made at the same locations as U and, whenever available, measurements from both sides of the tube center are plotted as open and filled symbols in Figures 16-24. As expected, the results show that the jet flow is not only axisymmetric in the mean, but also in the turbulence field. The w' measurements are not available for all x/D_j locations. They are obtained at selected locations to illustrate the similarity of the u' and w' distributions.

In general, the turbulence distributions are quite similar to those measured in the equilibrium region of free jets. The profiles peak at the jet centerline and decrease to some small finite value away from the jet. For flows through sudden expansions, one would expect to see a peak in the turbulence distributions at a radial position corresponding to the location of the separating streamline (Eaton and Johnston 1980). However, no such peaks are observed in any of the measured u'/U_o and w'/U_o profiles. This is a strong indication that the flow is jet-like rather than sudden-expansion-like. Further downstream, the turbulence field eventually evolves into a uniform distribution across the tube (Figure 18). At this point, the jet

has been completely dissipated, and the fluid in the tube moves with a fairly uniform velocity.

The turbulence profiles measured at $x/D_j \leq 2$ are essentially similar for all jet fluid densities and velocities. There are some exceptions, though. The u'/U_o and w'/U_o profiles for the helium/air jet at $U_j = 16.8$ m/s consistently peak at a higher level at the jet centerline. This difference even persists through the length of the jet. Since the measurements are consistent, they cannot be attributed to measurement errors. The reason for this difference is not known and could not be due to the fact that $\rho_j/\rho_a < 1$. Otherwise, one would expect to see the same behavior for the high velocity helium/air jet. Another anomaly is found in the air jet at $U_j \geq 152.8$ m/s. The u'/U_o profiles at $x/D_j = 1.25$ and 2 reveal that the peak occurs at about r = 6 mm, and resembles more closely the turbulence profiles of two-dimensional jets. This discrepancy could be attributed to measurement errors due to high shear gradient in this region. However, the data is too consistent for this to be true. One possible explanation could be the high turbulence production rate arising from the steep velocity gradient for this jet. This high local production may be responsible for the observed off-centerline peaks in the u'/U_o profiles at these x/D_j locations. The explanation is made even more plausible by the fact that the off-centerline peaks disappear as the jet moves downstream.

Although the u'/U_o profiles are quite similar for all confined jets at $x/D_j \leq 2$, they are quite different for $x/D_j > 3$. At these downstream locations, the u'/U_o profiles for low velocity jets consistently peak at higher levels at the jet centerline than high velocity jets. The same is also true of the w'/U_o profiles. It seems that the difference is a function of the density ratio, ρ_j/ρ_a; being biggest for helium/air jets and least for

CO_2 jets. The difference does not only occur at the jet centerline but extends to over half the jet width. In the case of the helium/air jets, the difference extends to cover the whole width of the jet. The reason could lie in the diffusion to convection velocity ratio. For slower moving jets, this ratio is larger. If, in addition, the jet fluid is lighter than the surrounding air, gravitational buoyancy would help increase the diffusion of jet fluid away from the jet centerline. Consequently, mixing is enhanced and this leads to an increase in turbulence intensities.

In spite of all these differences, the measurements do show the equilibrium nature of the jet flow. This observation is even more convincingly illustrated when the u'/U_o and w'/U_o profiles at $x/D_j \leq 2$ are compared with the measurements of Wygnanski and Fiedler (1969) at $50 \leq x/D_j \leq 97.5$ for free air jets. These are plotted with u'/U_o and w'/U_o versus $r/r_{1/2}$ in Figures 25 and 26. The mean lines through Wygnanski and Fiedler's data are represented by solid curves. This comparison clearly shows that the confined jets have achieved a self-preserving state even at $x/D_j = 1.25$, and that the turbulence field is in local equilibrium with striking similarity to those found in free jet flows.

Altogether, the evidence presented clearly indicates that dissipation due to work done on the stationary fluid column plays an important role in bringing the confined gas jets into local equilibrium. This effect overwhelms the influence of all other parameters, such as pressure gradient, ρ_j/ρ_a and $\dot{M}_j$. Consequently, the initial behavior of confined gas jets is essentially the same for all jet fluid densities and velocities investigated.

4. Conclusions

Based on the results presented in Section 3, the following conclusions can be drawn. These are:

(1) Confined gas jets are highly dissipative.

(2) More than 60% of the initial jet momentum is lost in the first diameter downstream of the jet.

(3) One consequence of this highly dissipative phenomenon is the rapid approach of the jet to a local equilibrium state. The resulting turbulence field bears striking resemblance to that found in the self-preserving region of free air jets.

(4) Dissipation due to work done by the jet essentially dominates the behavior in the initial region of the jets. Its influence overwhelms all other effects due to such parameters as Reynolds number, pressure gradient, density ratio, jet momentum, etc.

(5) Thereafter, the jets persist in a state of local equilibrium and the resultant mean velocity profiles can be adequately described by $U/U_o = e^{-\xi^2 \ln 2}$ for all x locations, jet fluid densities and velocities.

(6) The jets decay rapidly. In all the cases studied, the jet is found to be completely dissipated in ~ 30 jet diameters, thus giving rise to a uniform flow with a very high but constant turbulence field across the confinement.

(7) The jet centerline velocity obeys a power-law decay.

(8) The exponent is found to be a function of ρ_j/ρ_a only when $\rho_j/\rho_a > 1$. For jets with $\rho_j/\rho_a \leq 1$, there is no discernible difference in the power-law exponent. On the other hand, the exponent is a function of $\dot{M}_j$ for jets with $\rho_j/\rho_a \leq 1$.

(9) For all confined jets studied, the exponent is found to increase as the jets move downstream.

(10) Even though the jets are highly dissipative, the turbulence intensities are not as isotropic as those found in free jets. The ratio, u'_o/w'_o, is ~ 1.8 compared to ~ 1.2 found in free jets.

References

Abramovich, G. N., Yakovlevsky, O. V., Smirnova, I. P., Secundov, A. N. and Krashoninnikov, S. Yu. 1969. An investigation of the turbulent jets of different gases in a general stream. Astron. Acta. 14, 229-240.

Ahmed, S. A. and So, R. M. C. 1984. Concentration distributions in cylindrical combustors. In Experimental Measurements and Techniques in Turbulent Reactive and Non-Reactive Flows. Edited by R. M. C. So, J. H. Whitelaw, and M. Lapp. ASME Special Publication AMD-Vol. 66, 91-106.

Ahmed, S. A., So, R. M. C. and Mongia, H. C. 1985. Density effects on jet characteristics in confined swirling flow. Exp. in Fluids 3.

Alpinieri, L. J. 1964. Turbulent mixing of coaxial jets. AIAA J. 2, 1560-1567.

Becker, H. A., Hottel, H. C. and Williams, G. C. 1967. The nozzle-fluid concentration field of the round, turbulent, free jet. J. Fluid Mech. 30, 285-303.

Birch, A. D., Brown, D. R., Dodson, M. G. and Thomas, J. R. 1978. The turbulent concentration field of a methane jet. J. Fluid Mech. 88, 431-449.

Eaton, J. K. and Johnston, L. P. 1980. Turbulent flow reattachment: an experimental study of the flow and structure behind a backward-facing step. Rept MD-39, Thermo. Div., Stanford University.

Janjua, S. I., McLaughlin, D. K ., Jackson, T. W. and Lilley, D. G. 1983. Turbulence measurements in confined jets using a rotating single-wire probe technique. AIAA J. 21, 1609-1610.

Keagy, W. R. and Weller, A. E. 1949. A study of freely expanding inhomogeneous jets. Heat Transfer Fluid Mech. Inst., 89-98.

Maestrello, L. and McDaid, E. 1971. Acoustic characteristics of a high subsonic jet. AIAA J. 9, 1058-1066.

Schetz, J. A. 1980. Injection and mixing in turbulent flow. Progress in Astron. and Aero. 68, 39-51.

Sforza, P. M. and Mons, R. F. 1978. Mass momentum, and energy transport in turbulent free jets. Int. J. Heat Mass Transfer 21, 371-384.

So, R. M. C. and Liu, T. M. 1985. On self-preserving, variable-density, turbulent free jets. Submitted to ZAMP.

So, R. M. C., Ahmed, S. A. and Mongia, H. C. 1984. An experimental investigation of gas jets in confined swirling air flow. NASA CR-3832

So, R. M. C., Ahmed, S. A. and Mongia, H. C. 1985. Jet characteristics in confined swirling flow. Exp. in Fluids 3.

Way, J. and Libby, P. A. 1971. Application of hot-wire anemometry and digital techniques to measurements in a turbulent helium jet. AIAA J. 9, 1567-1573.

Wygnanski, I. and Fiedler, H. 1969. Some measurements in the self-preserving jet. J. Fluid Mech. 38, 577-612.

Zakkay, V., Krause, E. and Woo, S. D. L. 1964. Turbulent transport properties for axisymmetric heterogeneous mixing. AIAA J. 2, 1939-1947.

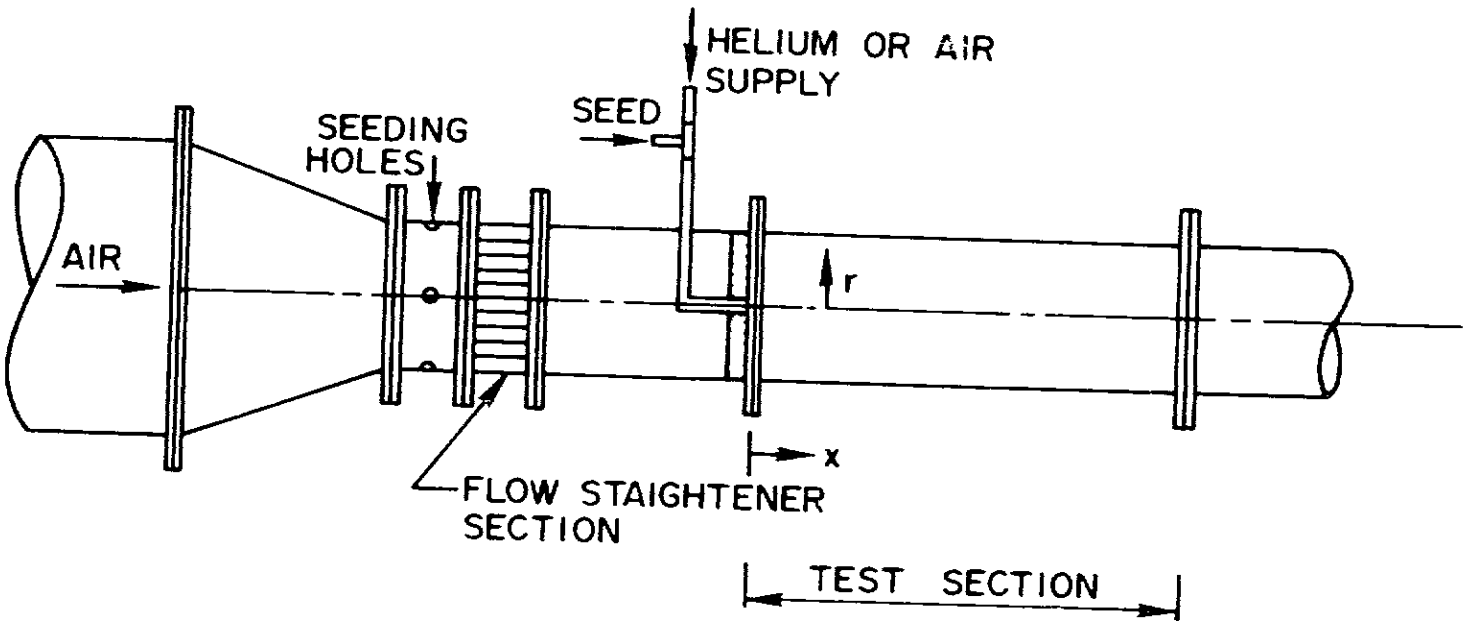

Figure 1. Schematic of facility test section.

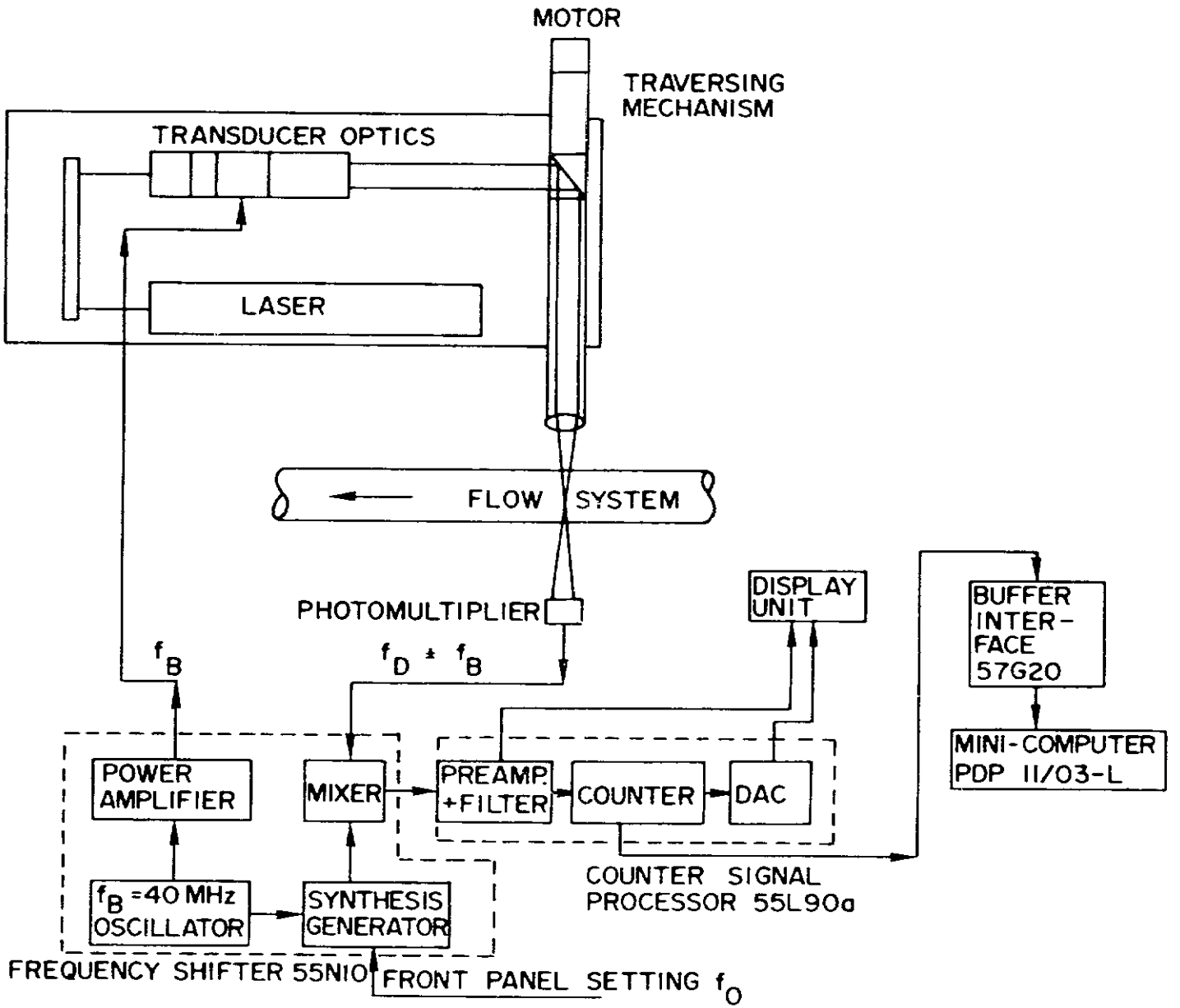

Figure 2. Block diagram of the LDA and data acquisition system.

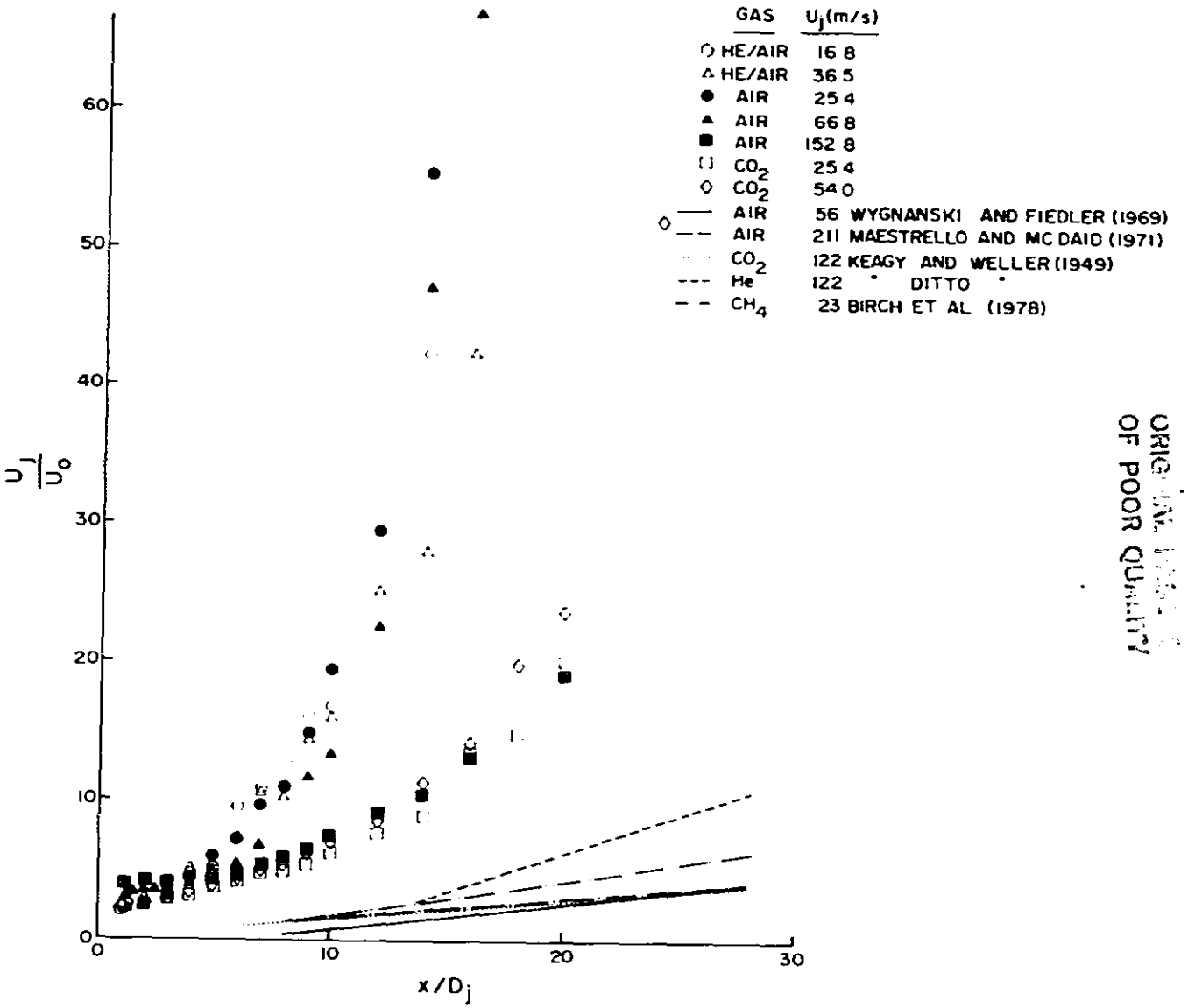

Figure 3. Centerline decay of mean aerial velocity for all jets tested.

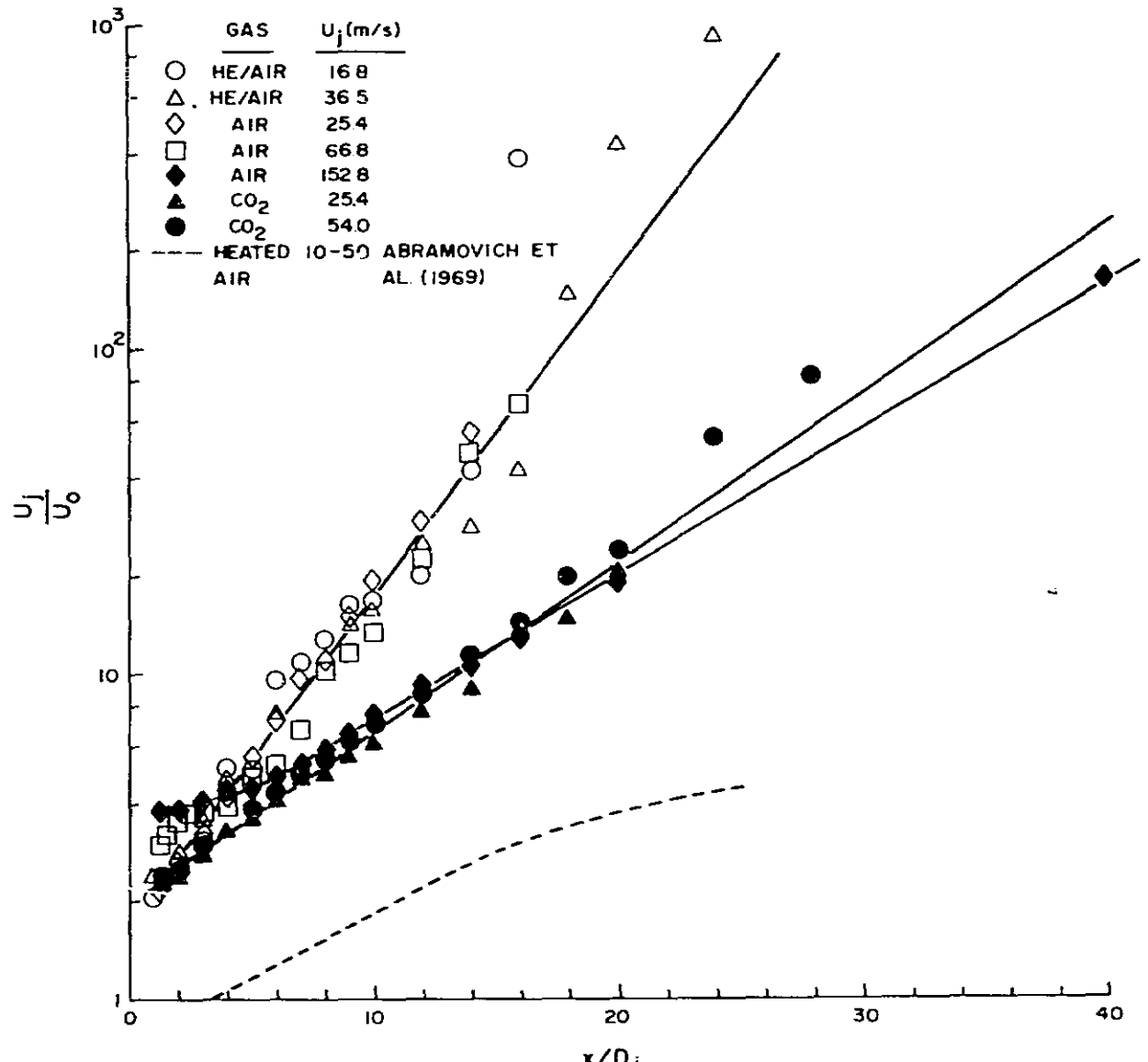

Figure 4. Semi-logarithmic plot of centerline velocity decay.

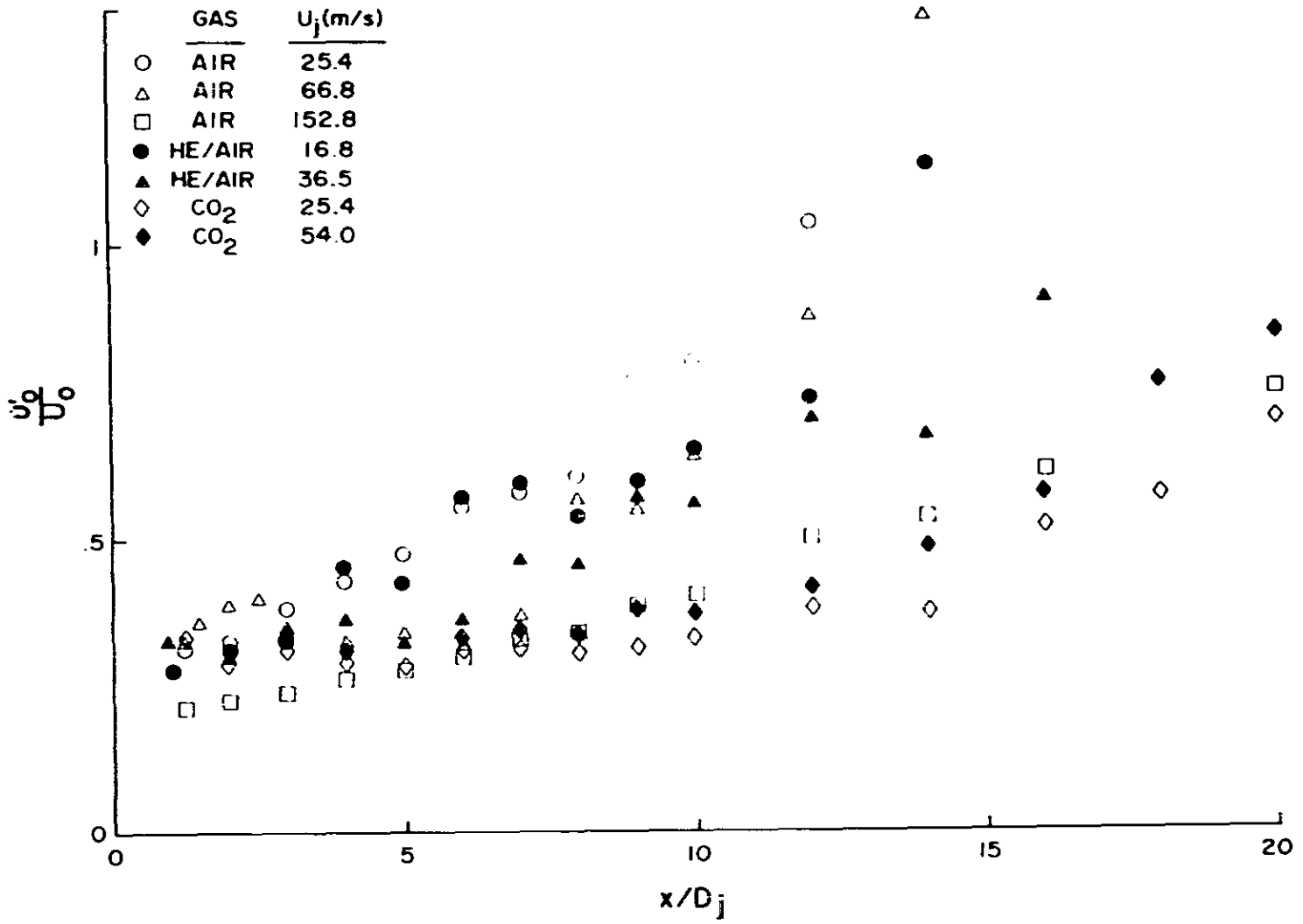

Figure 5. Centerline decay of u' for all jets tested.

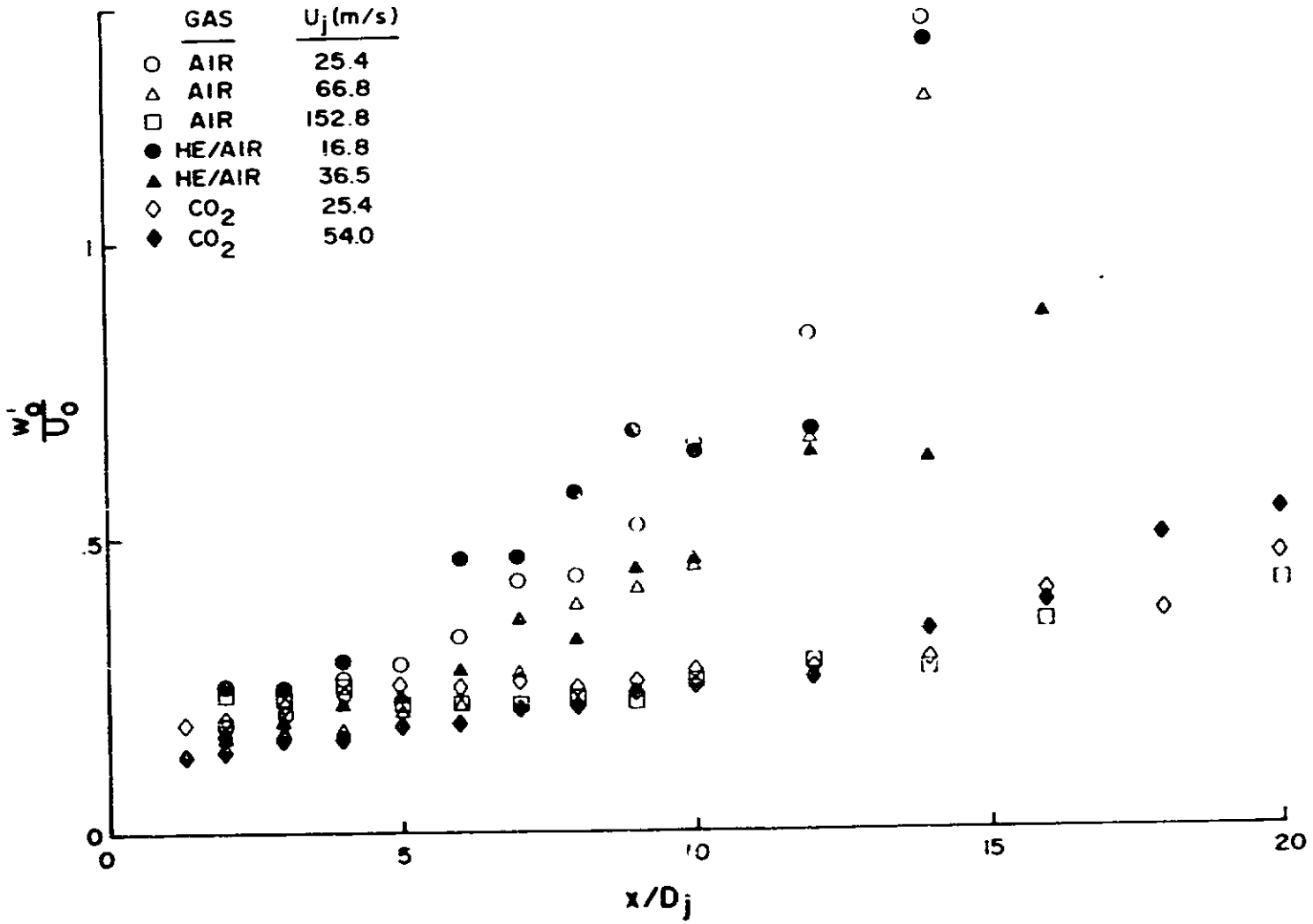

Figure 6. Centerline decay of w' for all jets tested.

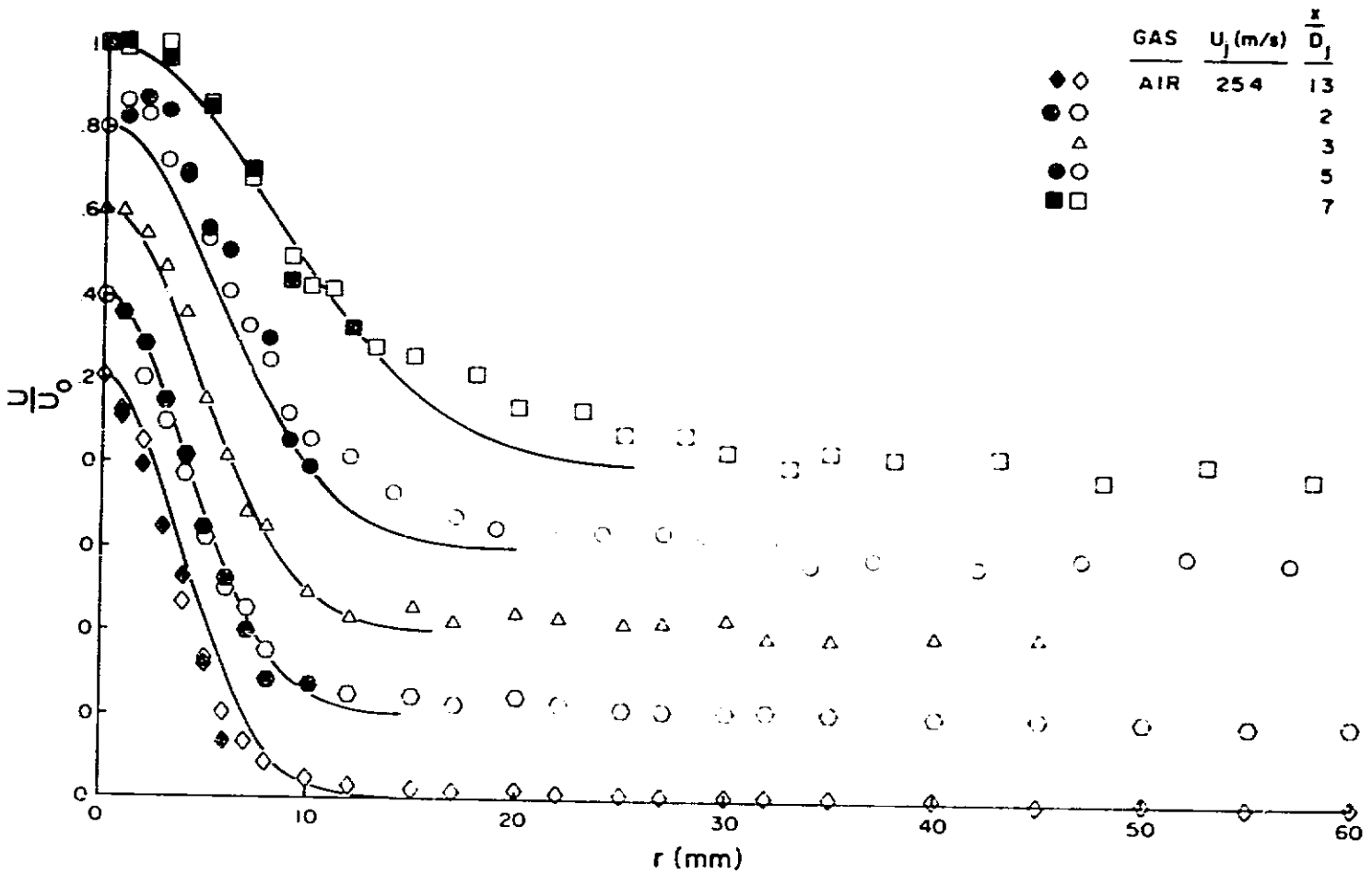

Figure 7. Evolution of U/U_o for air jet at U_j = 25.4 m/s.

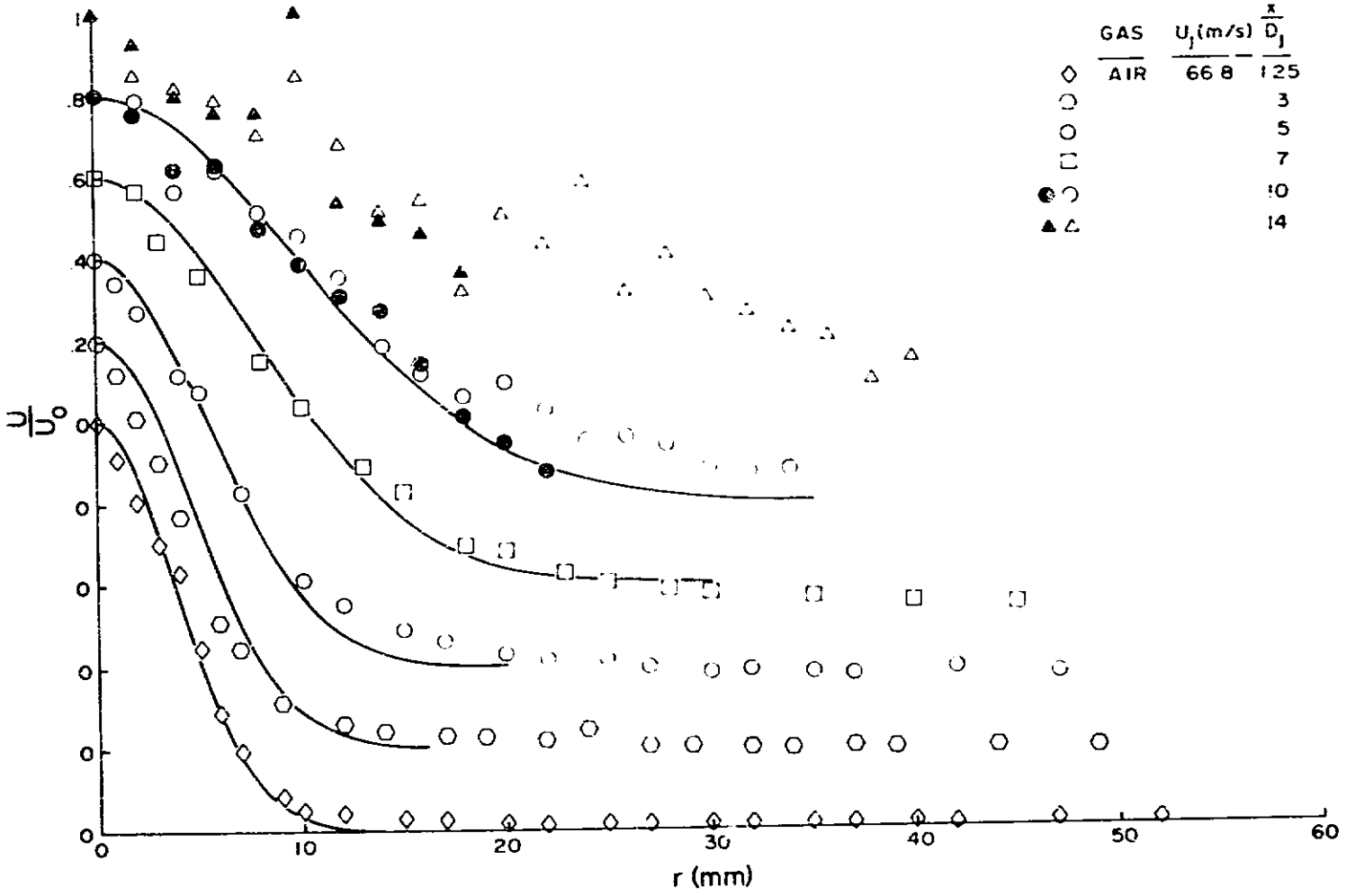

Figure 8. Evolution of U/U_o for air jet at U_j = 66.8 m/s.

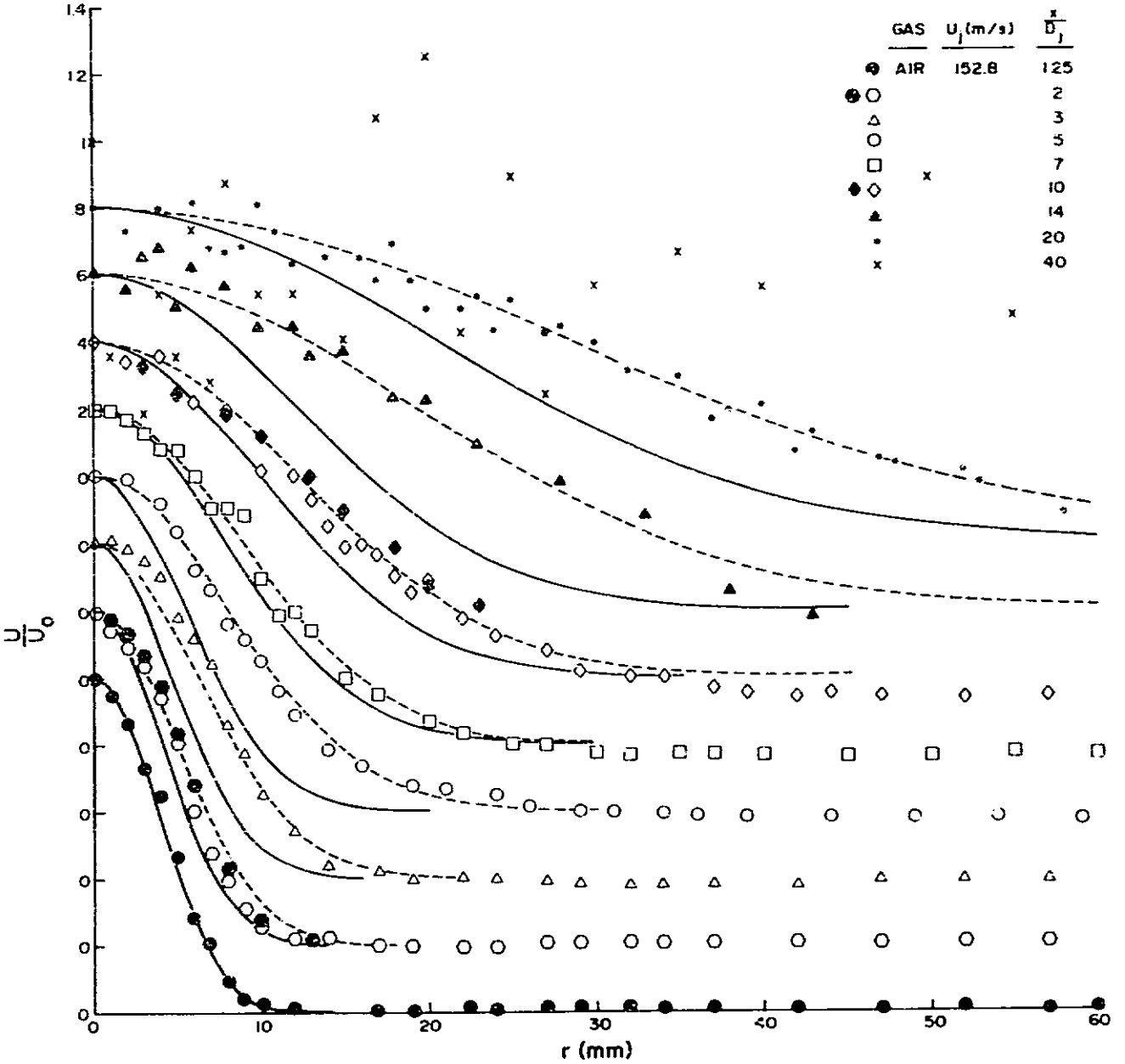

Figure 9. Evolution of U/U_o for air jet at U_j = 152.8 m/s.

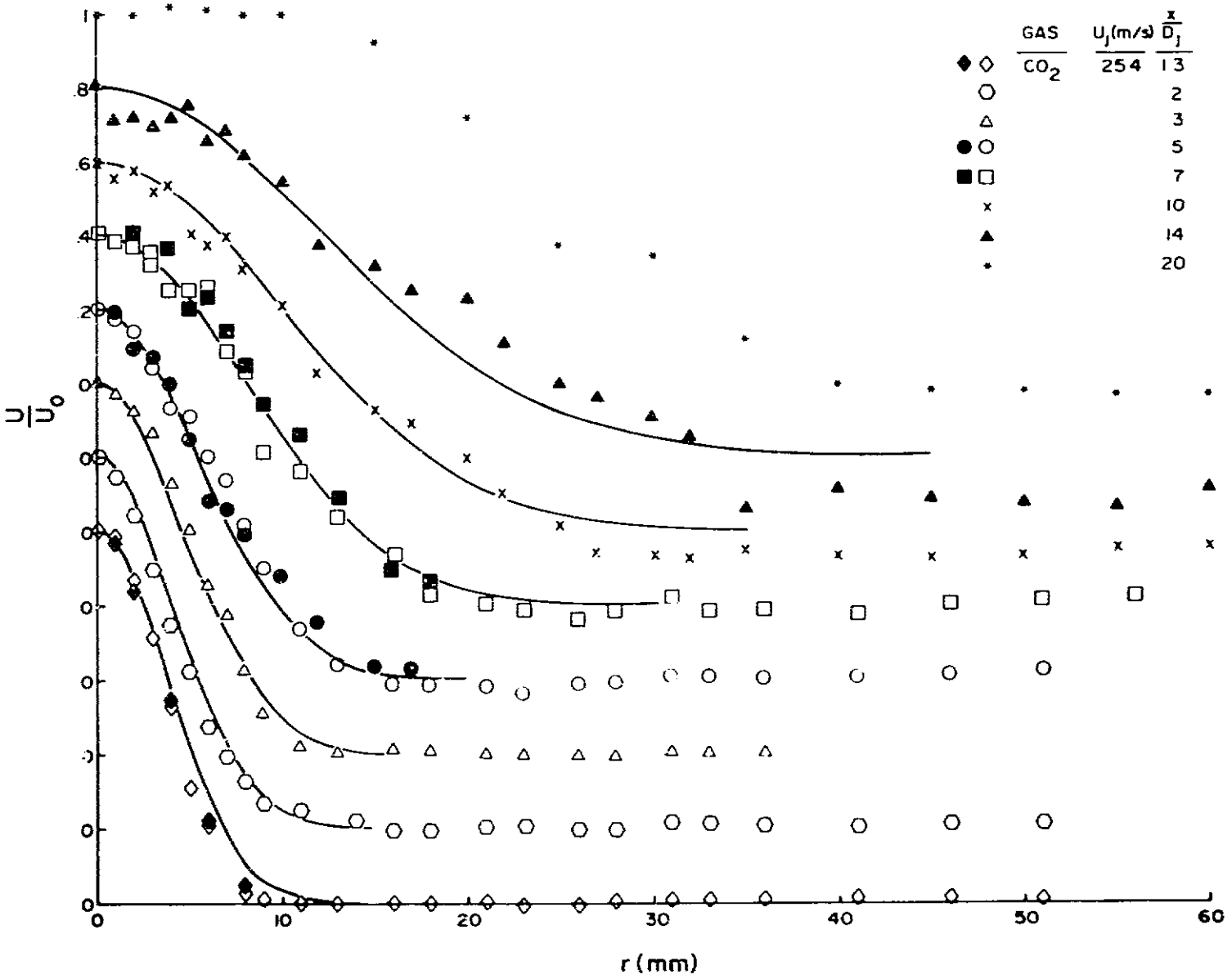

Figure 10. Evolution of U/U_o for CO_2 jet at U_j = 25.4 m/s.

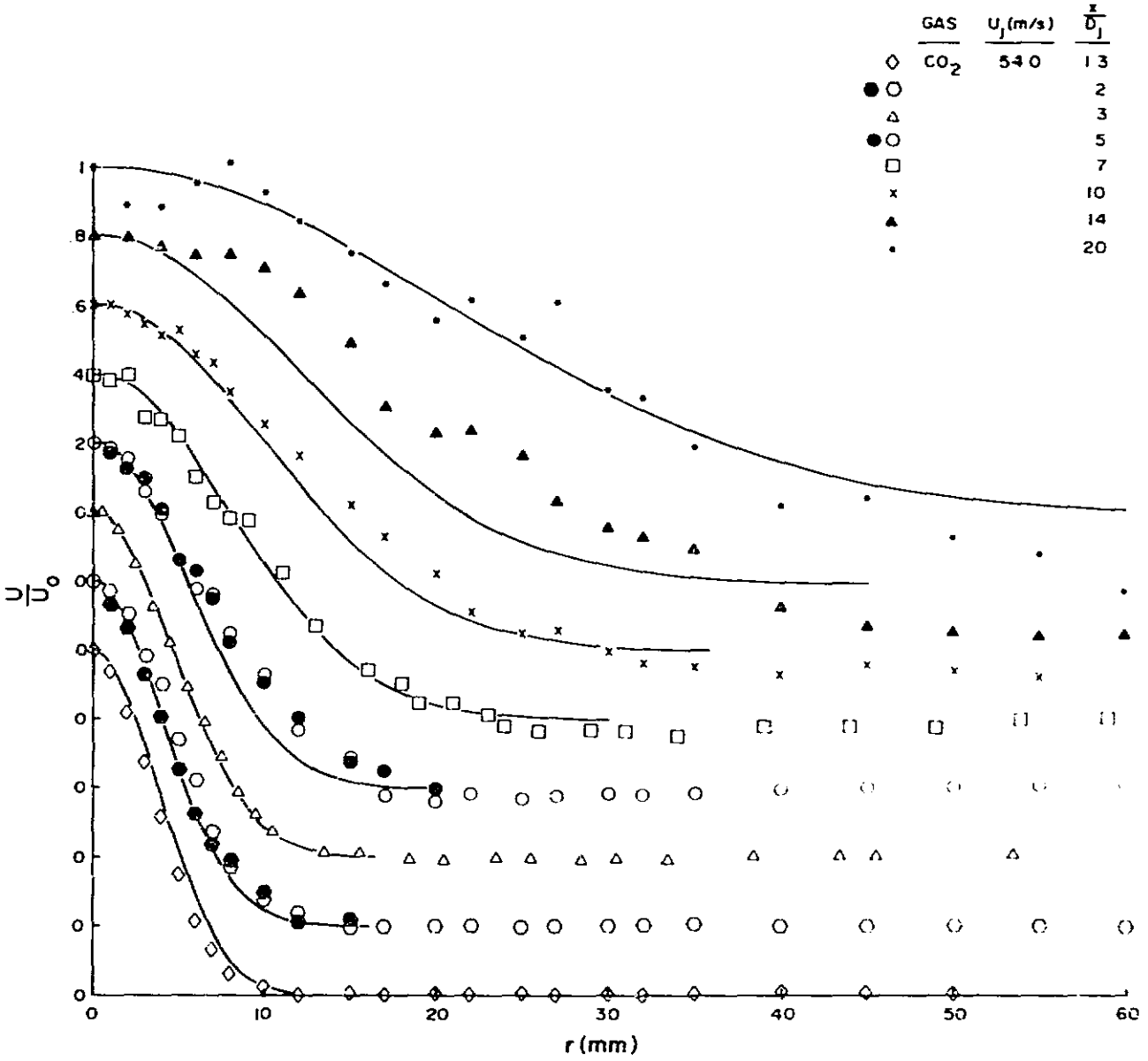

Figure 11. Evolution of U/U_o for CO_2 jet at U_j = 54.0 m/s.

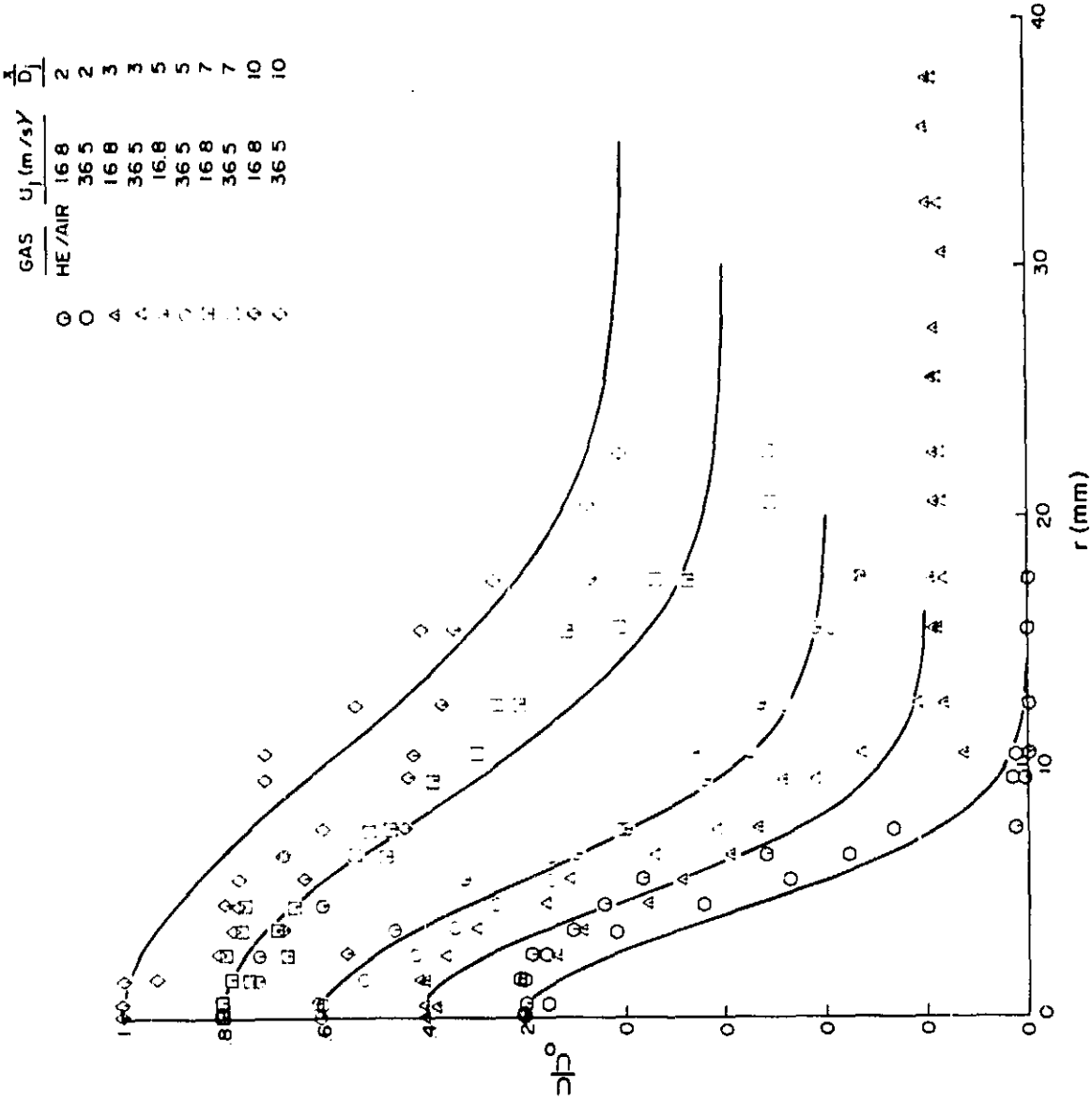

Figure 12. Evolution of U/U_o for He/air jets at U_j = 16.8 and 36.5 m/s.

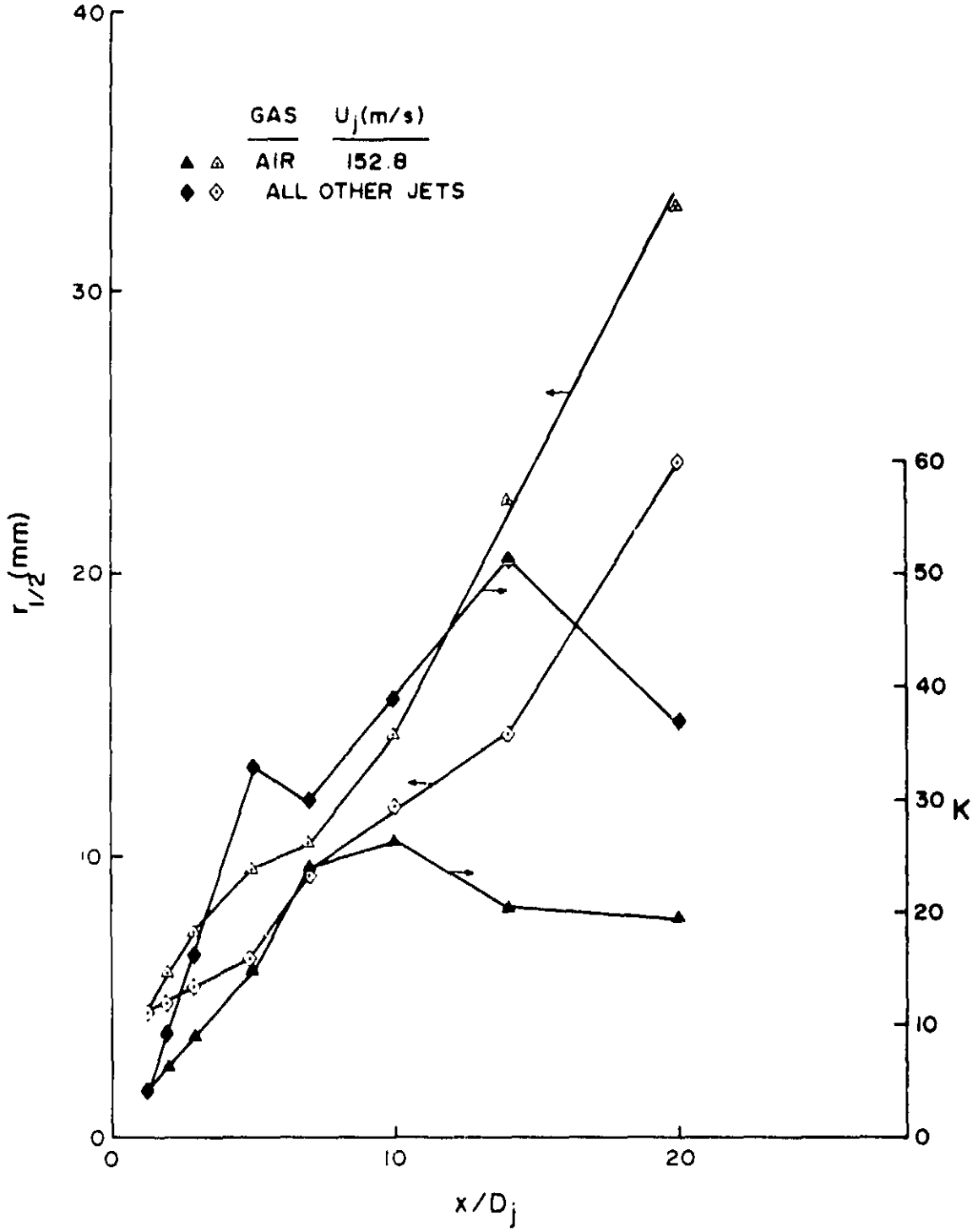

Figure 13. A plot of $r_{1/2}(x)$ and $K(x)$ vs. x/D_j for all jets tested.

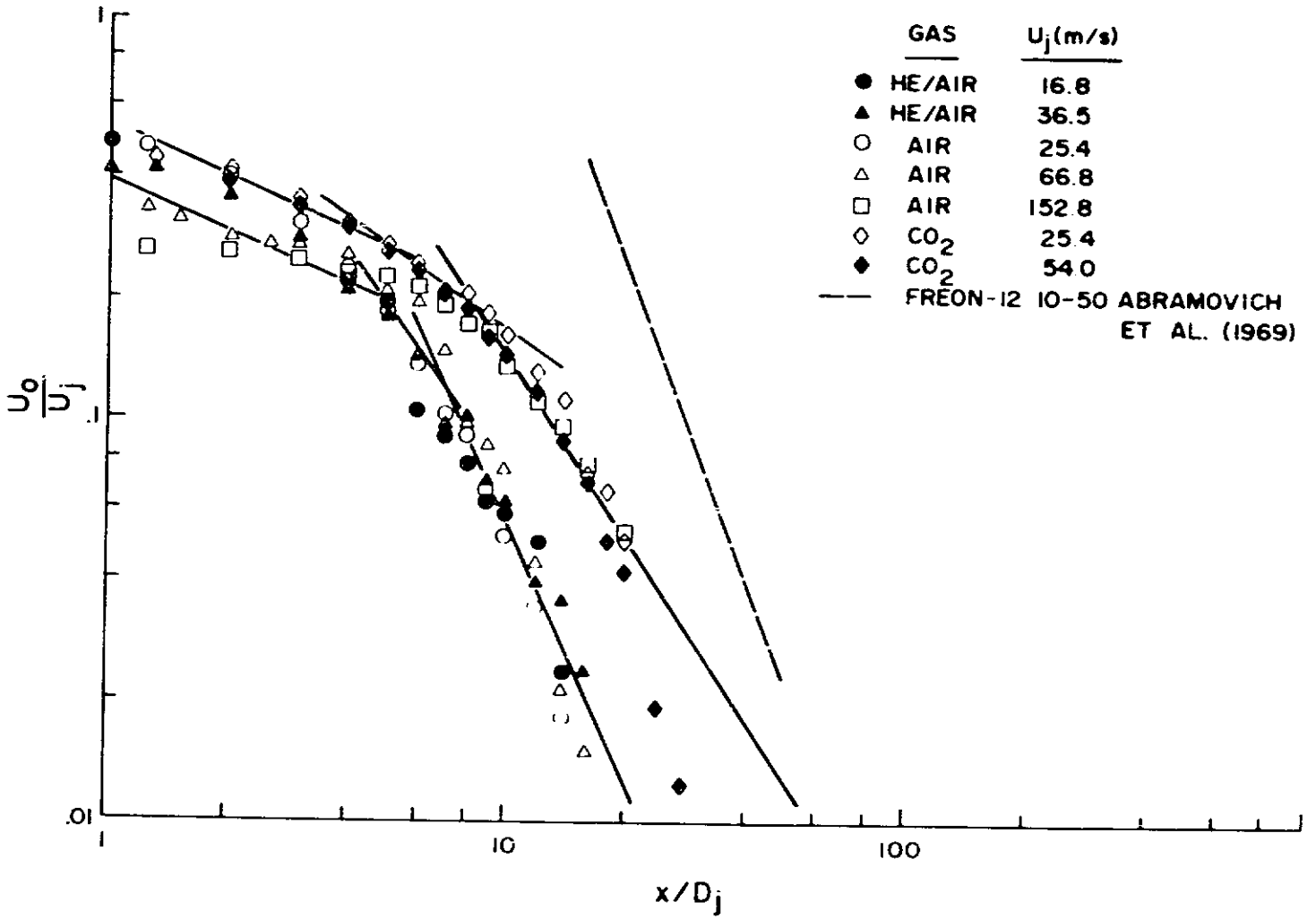

Figure 14. A plot to show the power law decay of jet centerline velocity.

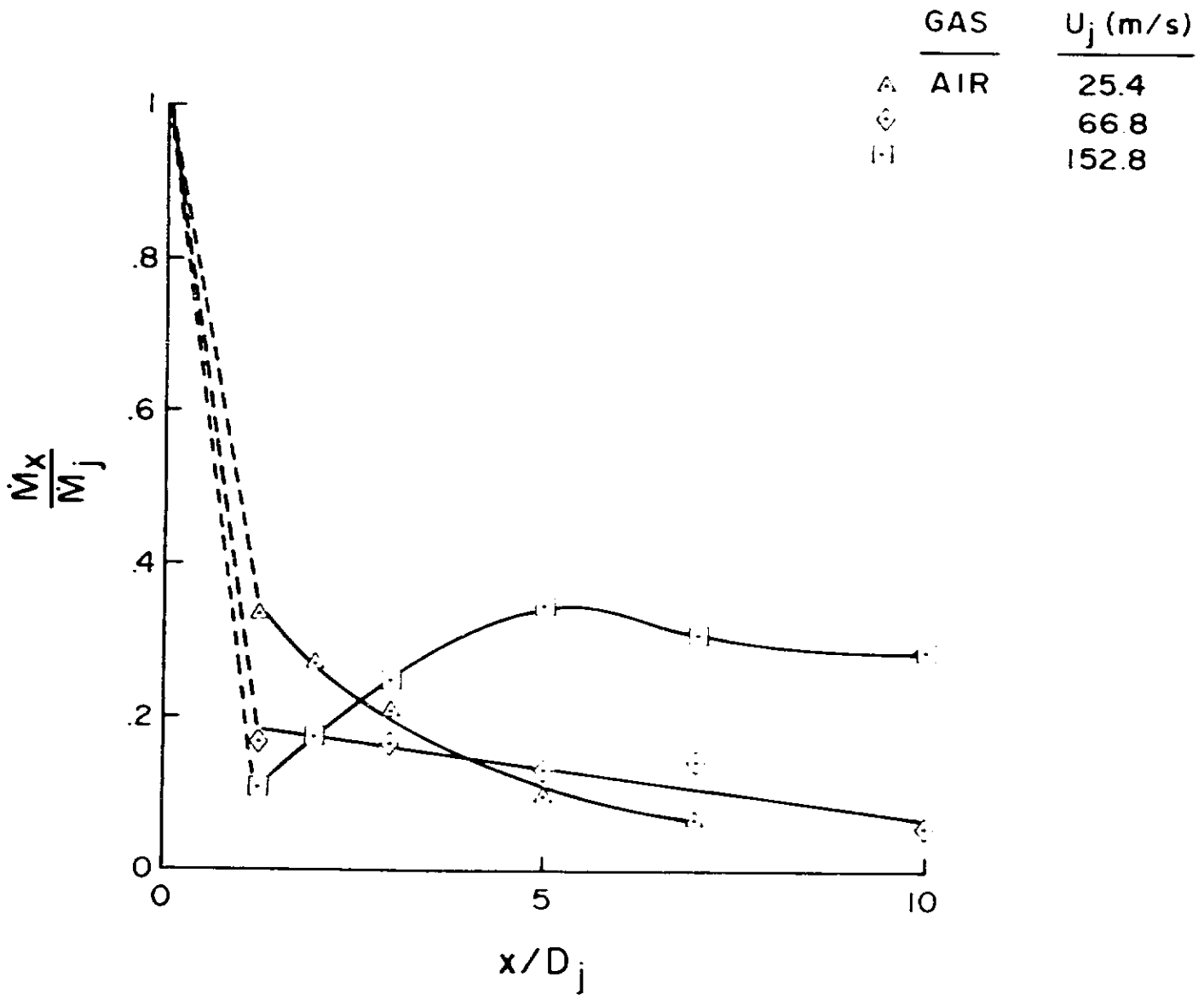

Figure 15. Decay of air jet momentum with x/D_j.

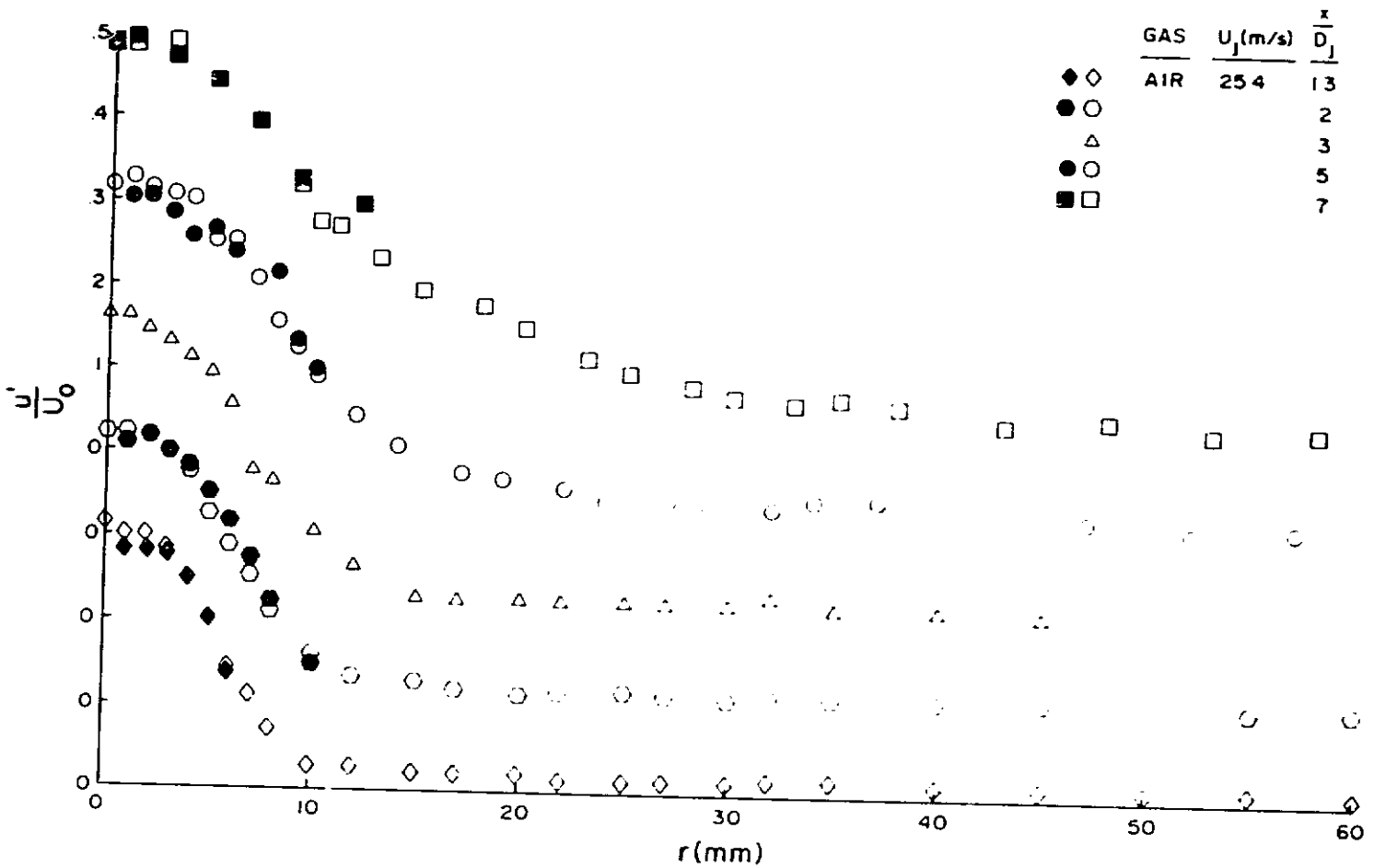

Figure 16. Evolution of u'/U_o for air jet at U_j = 25.4 m/s.

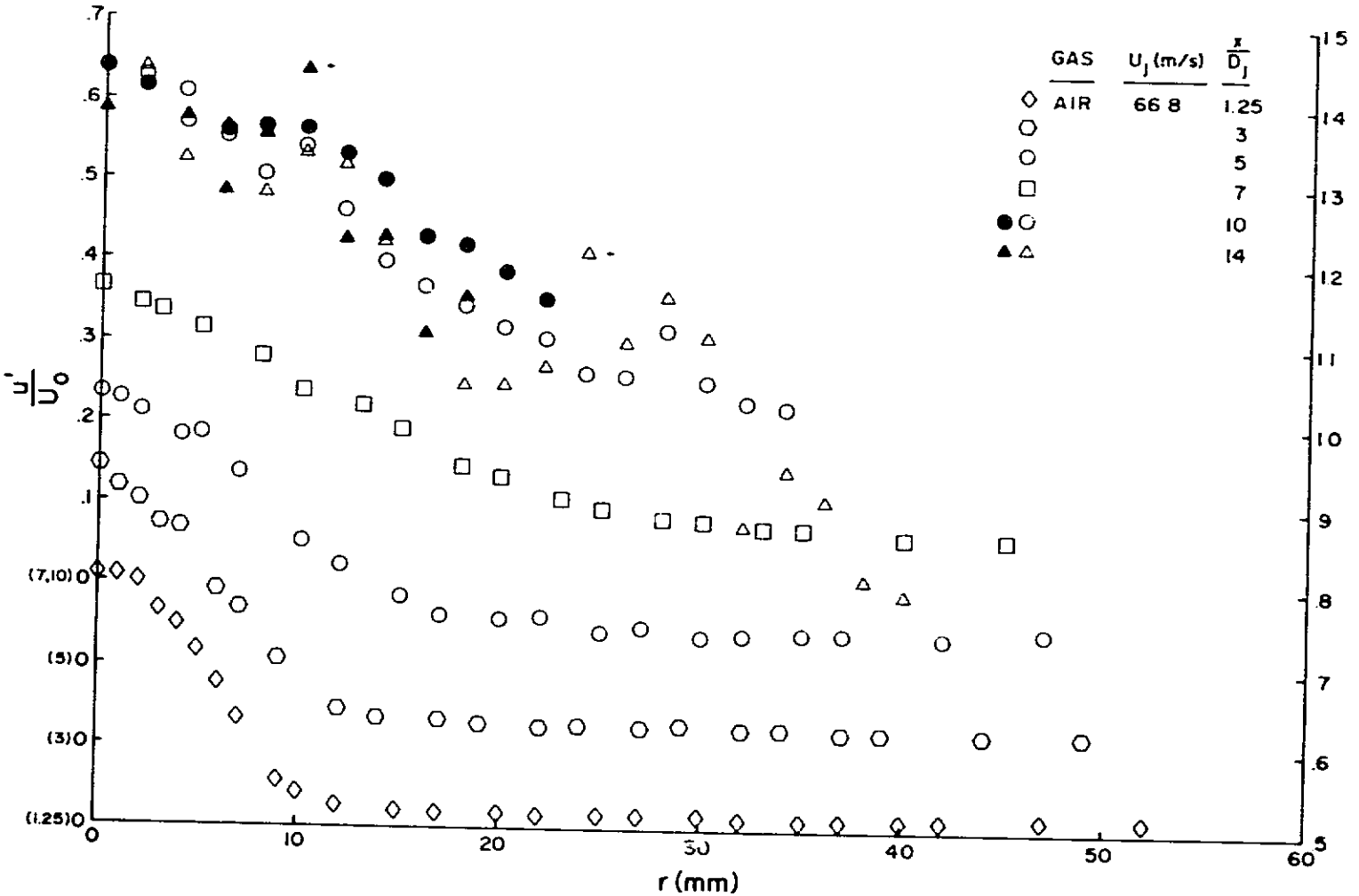

Figure 17. Evolution of u'/U_o for air jet at U_j = 66.8 m/s.

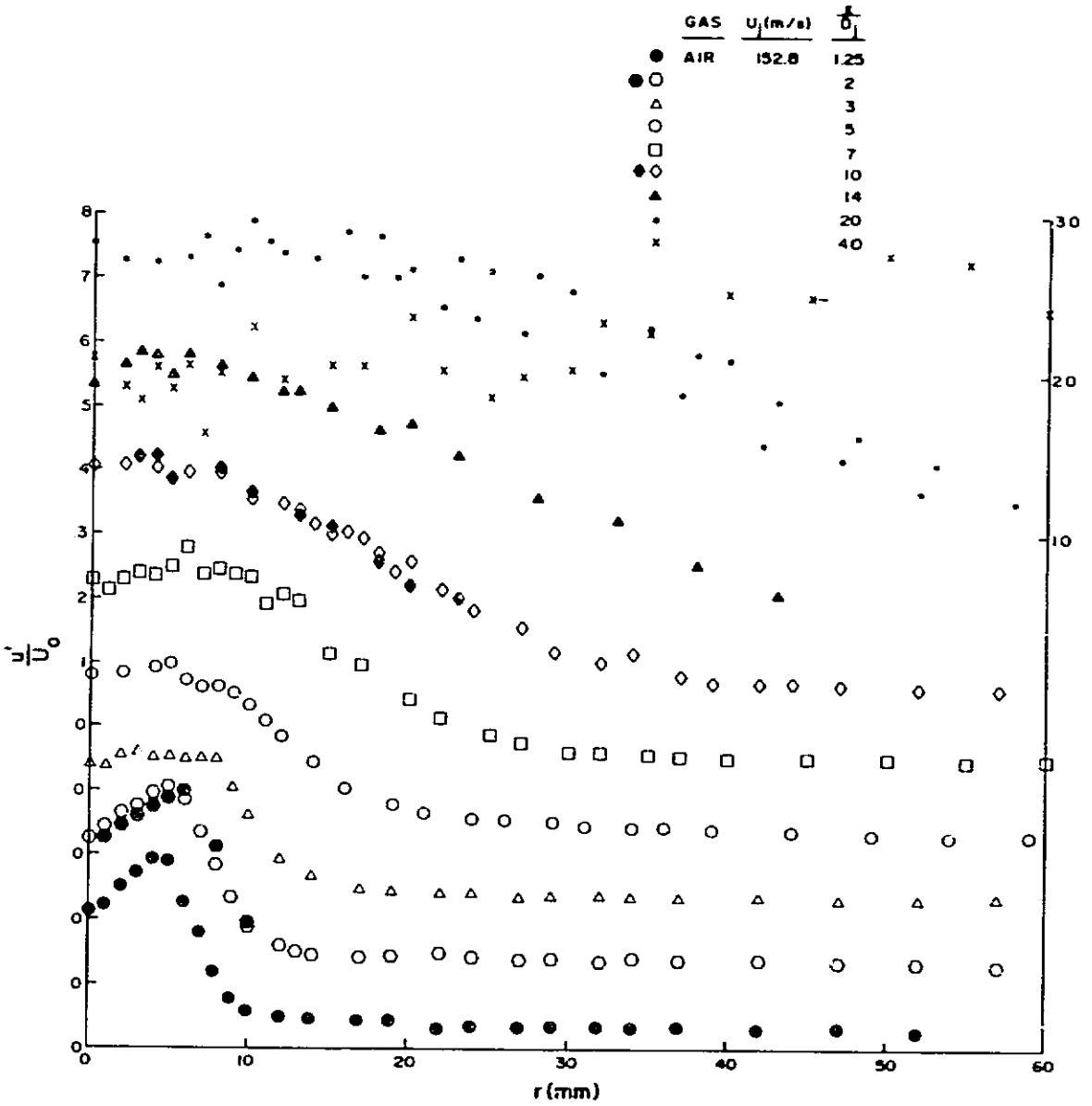

Figure 18. Evolution of u'/U_o for air jet at U_j = 152.8 m/s.

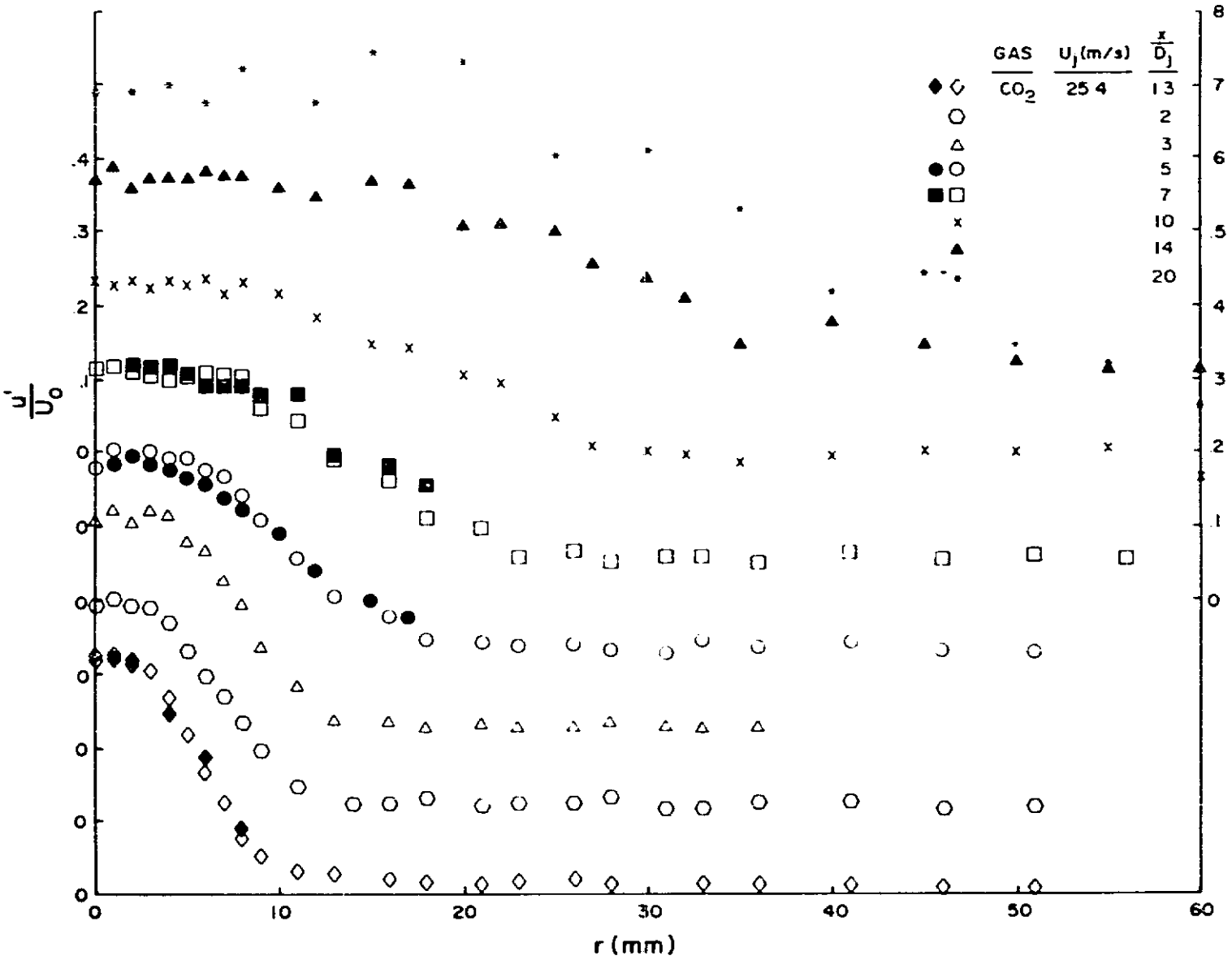

Figure 19. Evolution of u'/U_o for CO_2 jet at U_j = 25.4 m/s.

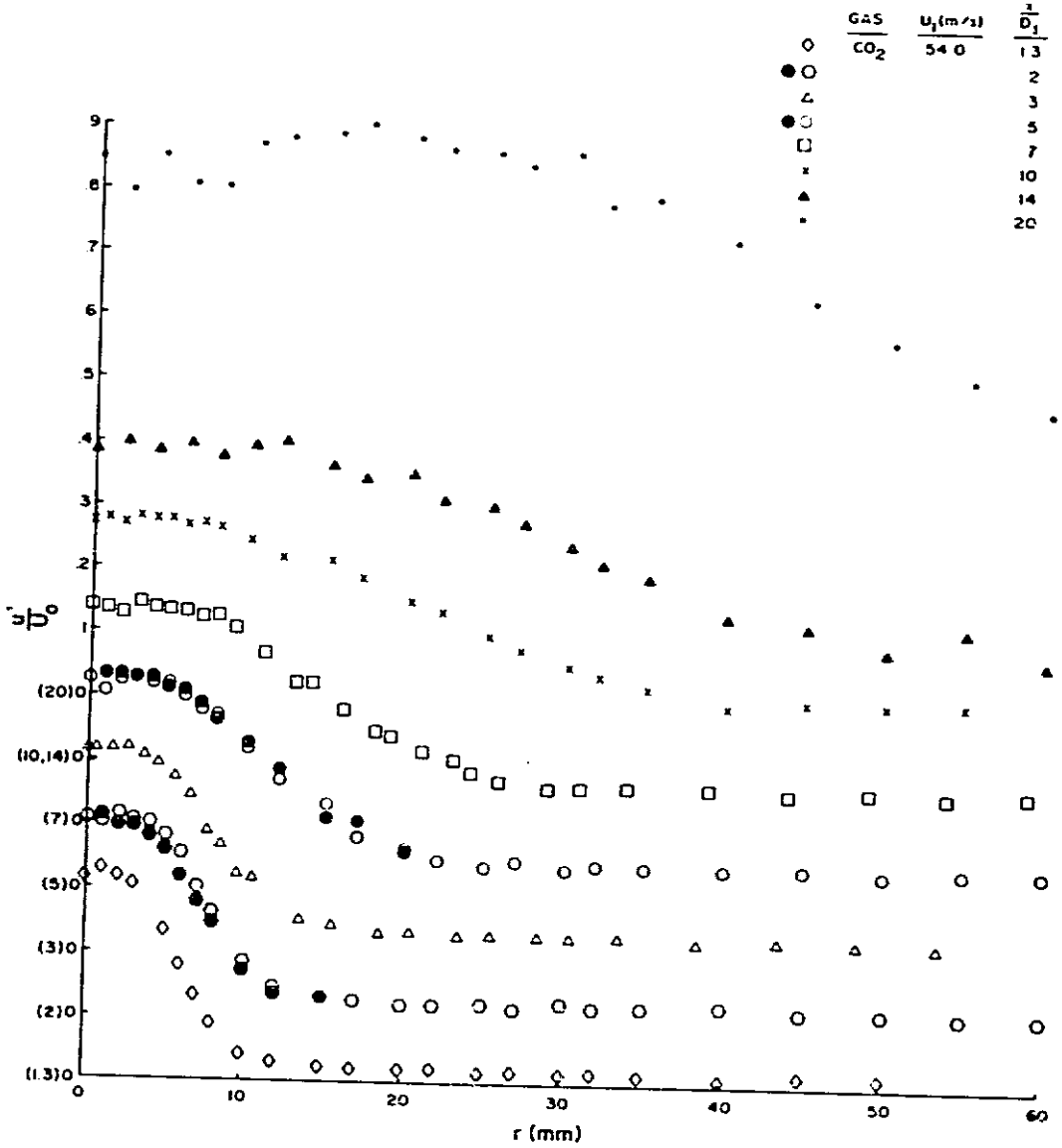

Figure 20. Evolution of u'/U_o for CO_2 jet at U_j = 54.0 m/s.

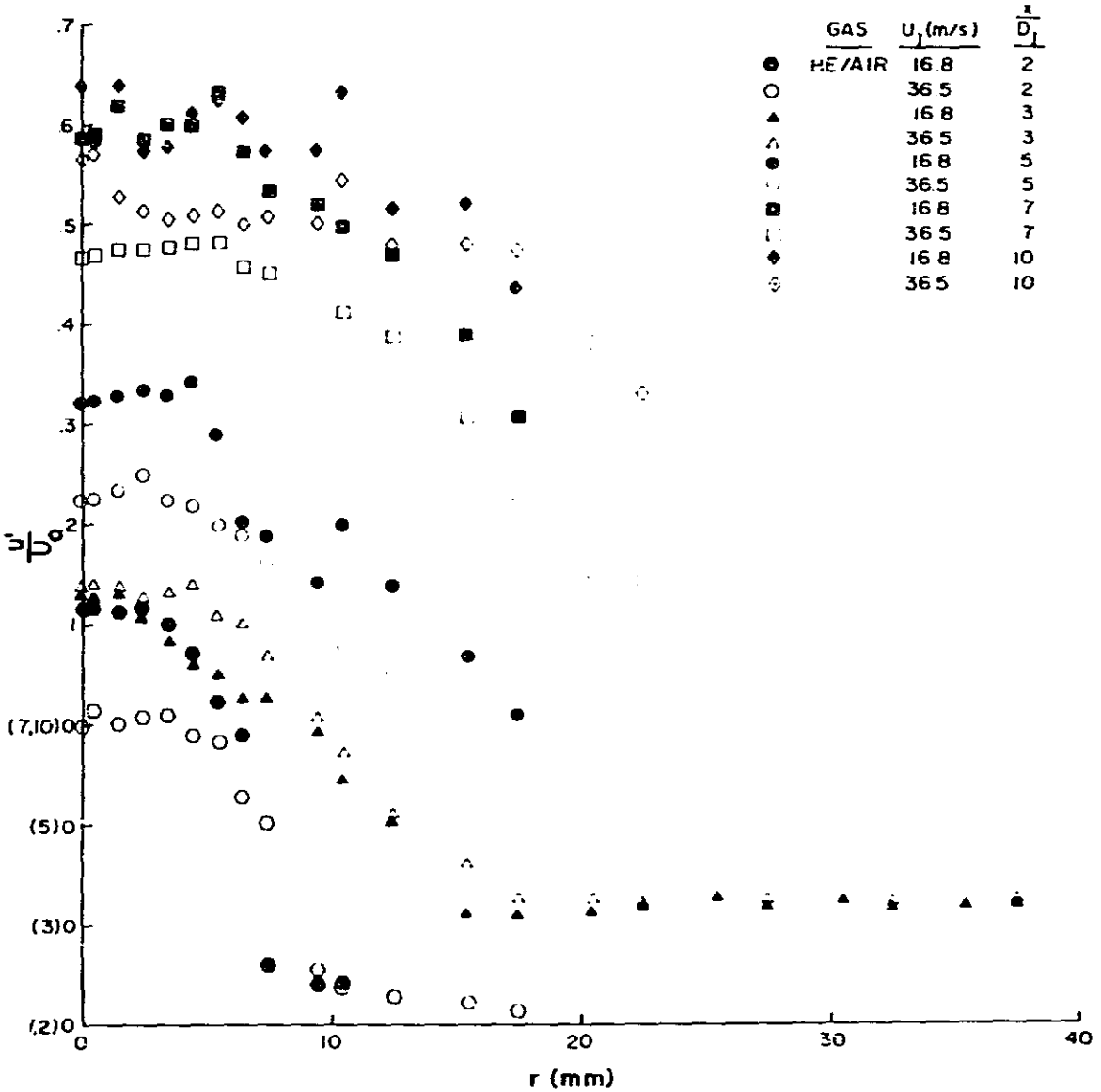

Figure 21. Evolution of u'/U_o for He/air jets at U_j = 16.8 and 36.5 m/s.

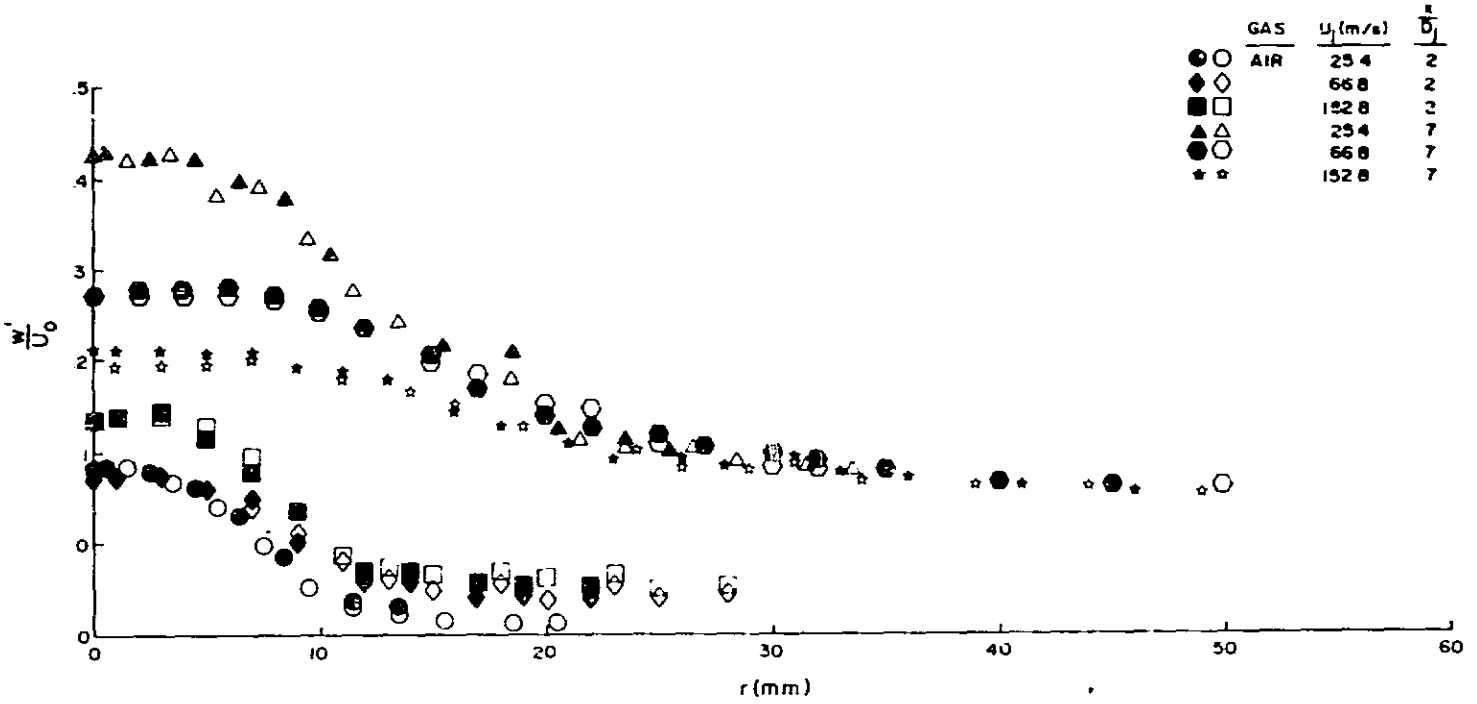

Figure 22. Profiles of w'/U_o at two x/D_j locations for all air jets.

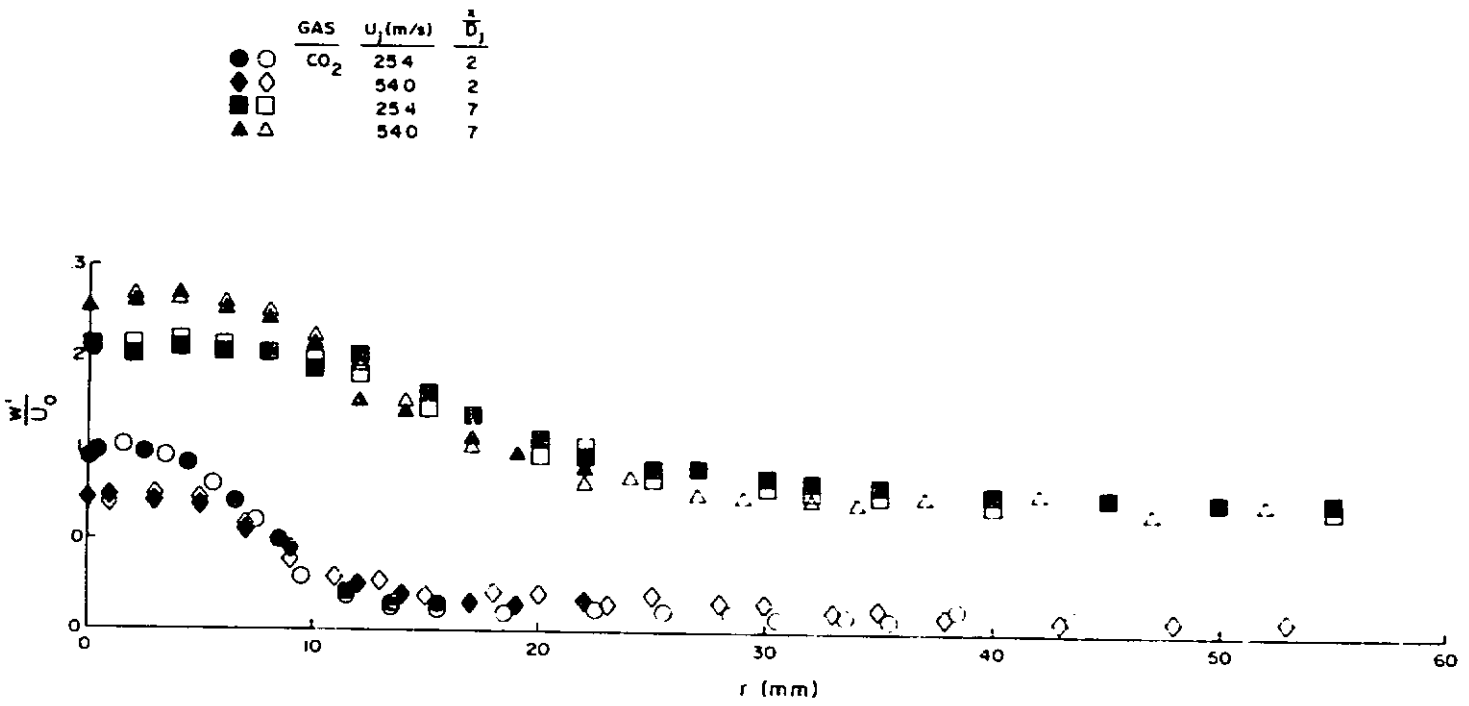

Figure 23. Profiles of w'/U_o at two x/D_j locations for all CO_2 jets.

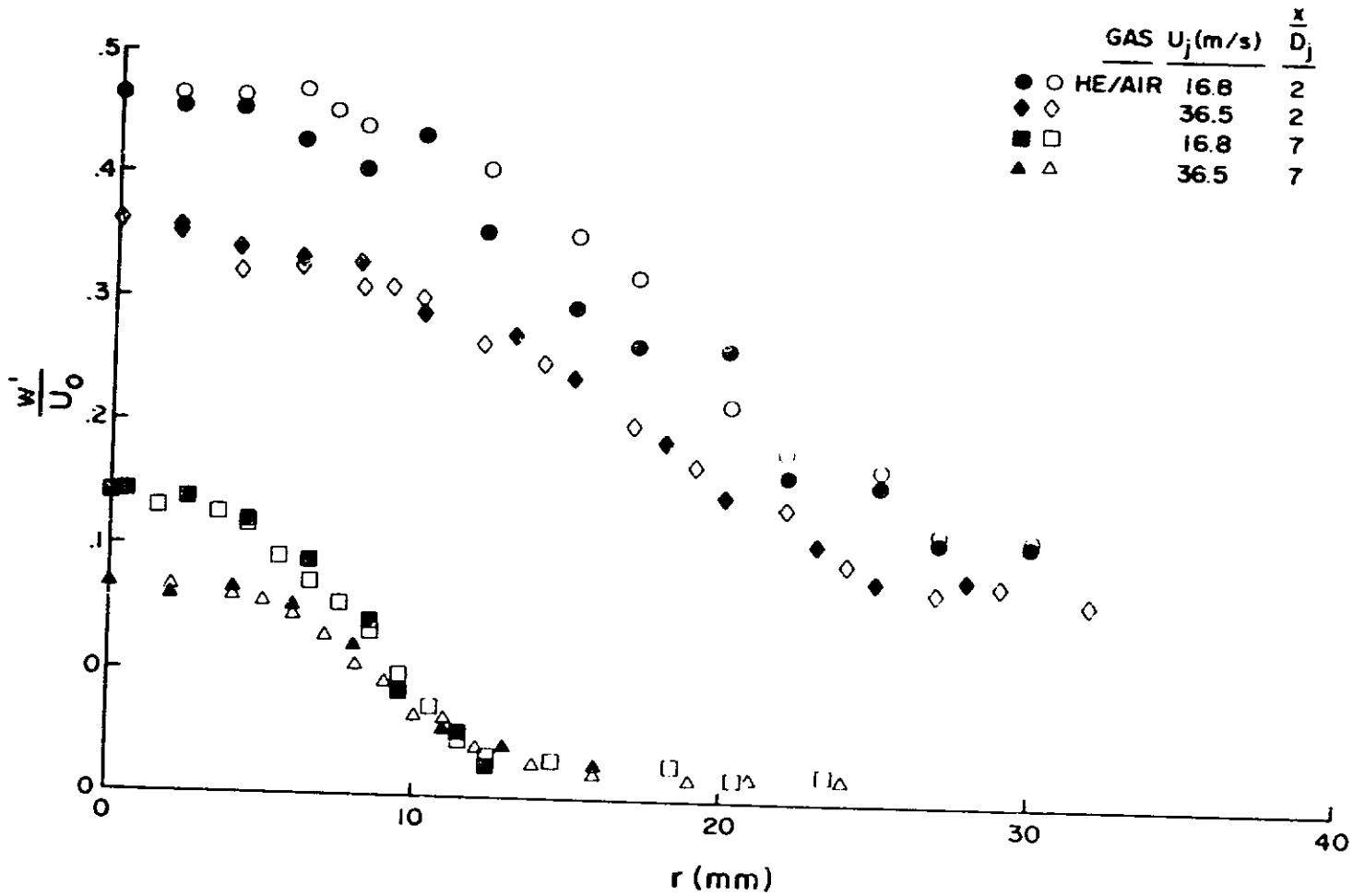

Figure 24. Profiles of w'/U_o at two x/D_j locations for all He/air jets.

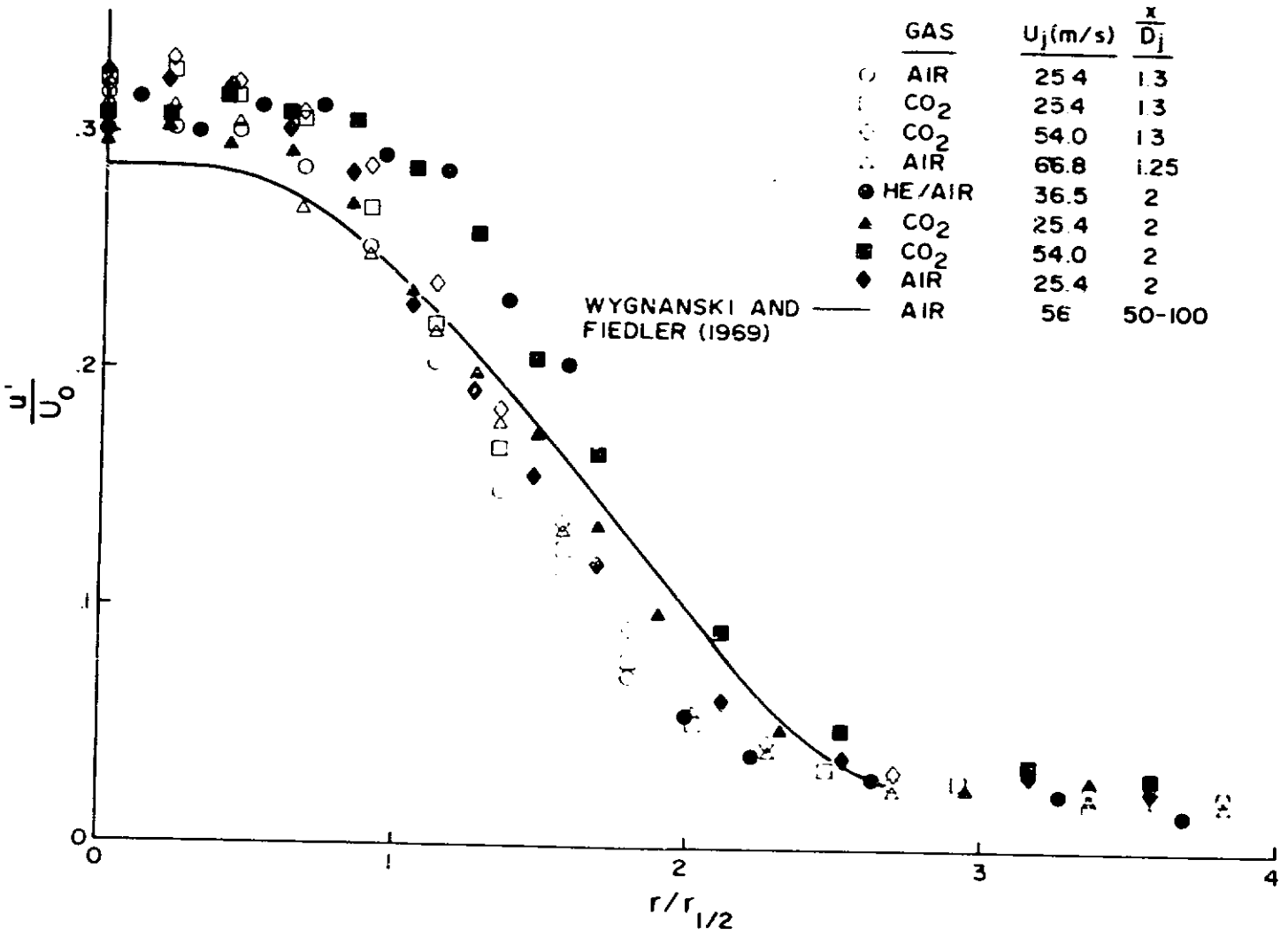

Figure 25. A comparison of the turbulence profiles, u'/U_o, at $x/D_j \leq 2$ with four air jet measurements at $x/D_j > 50$.

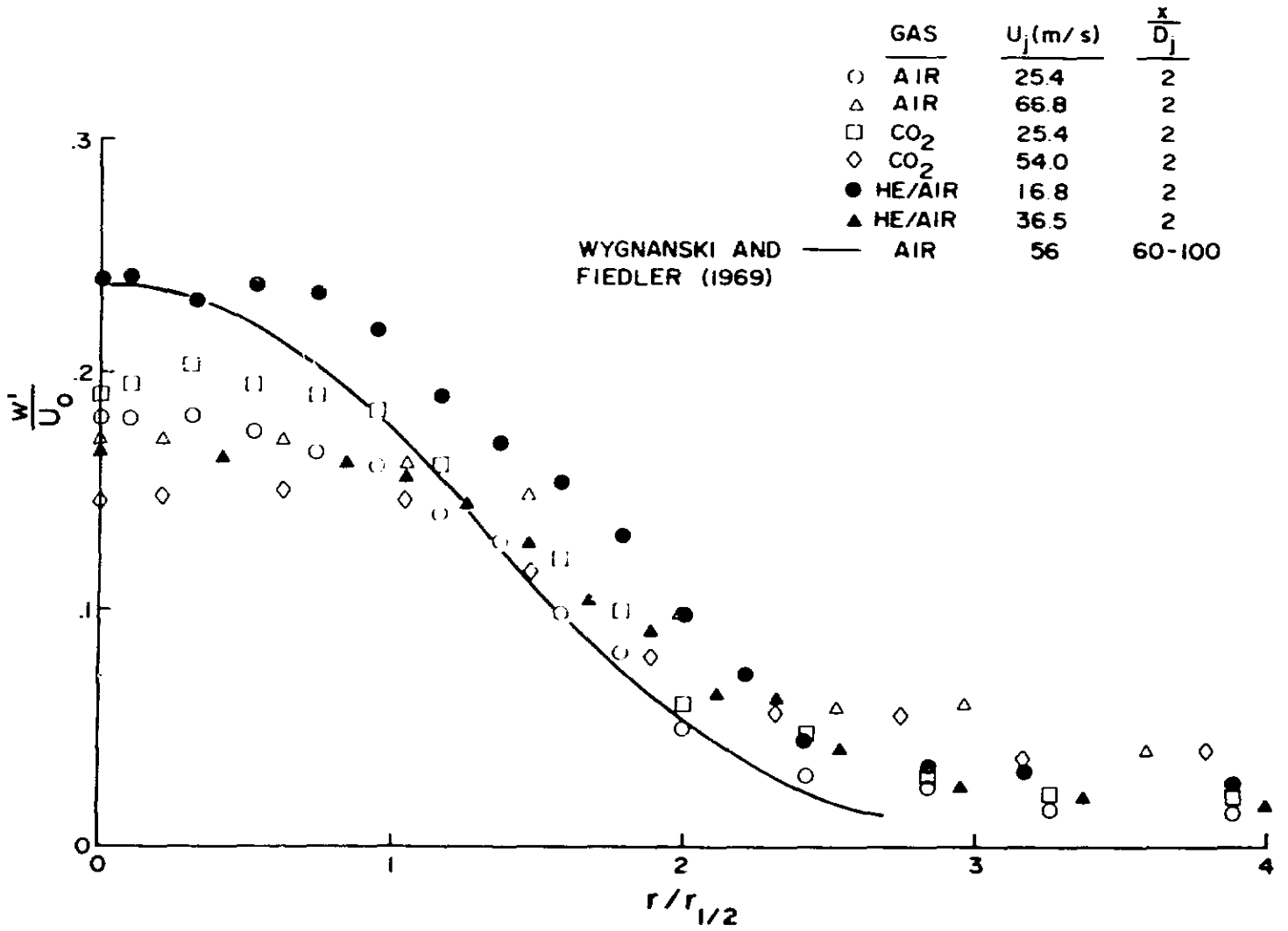

Figure 26. A comparison of the turbulence profiles, w'/U_o, at $x/D_j = 2$ with four air jet measurements at $x/D_j > 60$.

TABLE OF RESULTS

Table 1. Test Conditions of Confined Jets.

Parameters	Carbon Dioxide		Air			Helium/Air	
ρ_j/ρ_a	1.52	1.52	1	1	1	.31	.23
U_j (m/s)	25.4	54.0	25.4	66.8	152.8	16.8	36.5
$Re_j x10^{-3}$	28.43	60.44	14.38	37.82	86.51	1.50	2.97
$\dot{M}_j/\dot{M}_r$	.220	.993	.144	1	5.23	.020	.068

Table 2. Centreline Decay of Carbon Dioxide Jets.

$\frac{x}{D_j}$	U_j = 25.4 m/s			U_j = 54 m/s		
	U_o(m/s)	u'_o(m/s)	w'_o(m/s)	U_o(m/s)	u'_o(m/s)	w'_o(m/s)
1.3	11.16	3.59	2.08	22.50	7.16	3.06
2	10.4	3.08	1.98	21.40	6.61	3.02
3	8.86	2.74	1.96	18.30	5.85	2.96
4	7.72	2.23	1.82	16.40	5.10	2.69
5	6.86	1.93	1.67	14.30	4.71	2.57
6	6.15	1.88	1.51	12.80	4.30	2.36
7	5.30	1.67	1.35	11.10	3.80	2.34
8	5.25	1.61	1.26	10.00	3.40	2.12
9	4.60	1.45	1.15	8.66	3.30	2.03
10	4.11	1.37	1.09	7.70	2.87	1.88
12	3.32	1.26	.92	6.30	2.64	1.67
14	2.85	1.06	.801	4.75	2.30	1.60
16	1.88	.980	.75	3.80	2.20	1.45
18	1.71	.980	.63	2.71	2.06	1.34
20	1.26	.880	.58	2.27	1.92	1.21
24			.47	1.04	1.70	.93
28			.43	.66	1.30	.86
32			.35			.82

Table 3. Centreline Decay of Air Jets.

$\frac{x}{D_j}$	U_j = 25.4 m/s			U_j = 66.8 m/s			U_j = 152.8 m/s		
	U_o(m/s)	u'_o(m/s)	w'_o(m/s)	U_o(m/s)	u'_o(m/s)	w'_o(m/s)	U_o(m/s)	u'_o(m/s)	w'_o(m/s)
1.25	–	–	–	22.20	6.94	–	40.26	8.57	–
1.30	11.98	3.78	–	–	–	–	–	–	–
1.50	–	–	–	20.80	7.50	–	–	–	–
2	10.12	3.28	1.83	19.00	7.35	3.25	39.6	8.91	9.4
2.50	–	–	–	18.11	7.16	–	–	–	–
3	7.78	2.97	1.59	18.16	6.24	3.08	37.9	9.10	8.66
4	6.00	2.56	1.51	17.10	5.50	2.89	35.2	9.20	8.53
5	4.61	2.19	1.30	13.81	4.60	2.89	34.5	9.70	7.63
6	3.50	1.94	1.16	12.80	4.10	2.78	32.3	9.80	6.98
7	2.62	1.52	1.11	9.93	3.64	2.69	29.6	9.70	6.20
8	2.31	1.40	.996	6.54	3.70	2.53	26.4	8.90	6.01
9	1.70	1.30	.88	5.74	3.11	2.35	24.6	9.23	5.52
10	1.30	1.04	.85	5.01	3.19	2.22	21.0	8.50	5.23
12	.86	.89	.72	2.96	2.60	1.96	16.8	8.40	4.67
14	.46	.76	.63	1.42	1.97	1.76	14.6	7.80	4.09
16			.54	1.00	1.71	1.65	11.6	7.10	4.06
18			.49			1.49	–	–	3.62
20			.41			1.43	8.00	6.00	3.27
24			.38			1.28	–	–	2.87
28			.33			1.02	–	–	2.50
32			.25			.89	–	–	2.39
36							–	–	2.27
40							.93	1.95	2.06

Table 4. Centreline Decay of Helium/Air Mixture Jets.

$\frac{x}{D_j}$	U_j = 16.8 m/s			U_j = 36.5 m/s		
	U_o(m/s)	u'_o(m/s)	w'_o(m/s)	U_o(m/s)	u'_o(m/s)	w'_o(m/s)
1	8.10	2.27	-	15.30	4.98	-
2	6.69	2.06	1.60	13.04	3.90	2.17
3	5.71	1.89	1.29	10.08	3.42	1.94
4	3.67	1.65	1.06	7.64	2.75	1.69
5	3.25	1.37	.87	6.64	2.16	1.50
6	1.76	.996	.82	5.03	1.82	1.39
7	1.55	.912	.72	3.42	1.60	1.23
8	1.31	.707	.75	3.62	1.68	1.15
9	1.04	.623	.70	2.52	1.44	1.12
10	.993	.635	.64	2.28	1.29	1.04
12	.834	.613	.56	1.45	1.02	.93
14	.398	.450	.53	1.30	.871	.81
16	.043	.390	.48	.862	.781	.75
18				.245	.738	.69
20				.086	.690	
24				.040	.463	

Table 5a. Velocity Measurements of Carbon Dioxide Jets at U_j = 25.4 m/s.

x/D_j	1.3	-			2	
4(mm)	U/U_o	U/U_o	u'/U_o	u'/U_o	U/U_o	u'/U_o
0	1.000	1.000	.322	.325	1.000	.296
1	.988	.970	.327	.320	.944	.301
2	.867	.835	.316	.321	.842	.293
3	.713	-	.306	-	.695	.291
4	.540	.534	.268	.249	.550	.270
5	.310	-	.218	-	.423	.232
6	.212	.224	.167	.185	.277	.197
7	.104	-	.124	-	.193	.172
8	.030	.056	.077	.086	.128	.135
9	.014		.053		.072	.097
11	0		.033		.049	.049
13	.001		.028		-	-
14	-		-		.021	.026
16	.001		.022		-.005	.027
18	-.002		.018		-.002	.033
21	.004		.015		.006	.022
23	-.008		.018		.007	.025
26	-.003		.022		-.007	.026
28	.006		.015		-.007	.033
31	.005		.009		.017	.018
33	.010		.016		.013	.017
36	.009		.014		.008	.025
41	.014		.013		.005	.025
46	.014		.009		.010	.015
51	.013		.010		.012	.019

Table 5b. Velocity Measurements of Carbon Dioxide Jets at U_j = 25.4 m/s.

x/D_j	2		3			5	
r(mm)	w'/U_o	w'/U_o	r(mm)	U/U_o	u'/U_o	U/U_o	u'/U_o
0	.190	.190	0	1.000	.309	1.000	.281
.5	-	.194	1	.971	.323	.972	.305
1.5	.203	-	2	.926	.305	.939	.296
2.5	-	.195	3	.865	.322	.840	.302
3.5	.190	-	4	.727	.315	.730	.292
4.5	-	.183	5	.606	.280	.706	.294
5.5	.160	-	6	.456	.266	.598	.277
6.5	-	.140	7	.374	.227	.536	.268
7.5	.121	-	8	.228	.196	.415	.242
8.5	-	.099	9	.108	.135	.296	.210
9.5	.060	-	11	.024	.084	.137	.159
11.5	.042	.041	13	.003	.037	.047	.106
13.5	.028	.028	16	.014	.036	-.010	.080
16.5	-	.028	18	.005	.027	-.012	.048
18.5	.021		21	0	.032	-.016	.045
20.5	.024		23	-.006	.028	-.036	.039
23.5	.023		26	-.001	.030	-.010	.042
25.5	.022		28	-.008	.036	-.004	.034
28.5	.020		31	.008	.030	.012	.031
30.5	.015		33	.002	.028	.009	.048
33.5	.018		36	.005	.030	.005	.037
35.5	.015		41			.013	.045
38.5	.020		46			.015	.032
43.5	.017		51			.028	.031
48.5	.016						
53.5	.016						
58.5	.015						

Table 5c. Velocity Measurements of Carbon Dioxide Jets at U_j = 25.4 m/s.

x/D_j	5		7				
r(mm)	U/U_o	u'/U_o	r(mm)	U/U_o	U/U_o	u'/U_o	u'/U_o
0	1.000	.281	0	1.000	1.000	.315	.315
1	.983	.284	1	.981	-	.317	-
2	.889	.297	2	.962	1.000	.317	.315
3	.867	.283	3	.943	.921	.315	.308
4	.790	.278	4	.849	.962	.301	.317
5	.643	.265	5	.842	.796	.308	.309
6	.481	.257	6	.855	.830	.309	.294
7	.453	.239	7	.681	.736	.306	.291
8	.389	.223	8	.638	.628	.302	.298
10	.280	.192	9	.408	.536	.262	.279
12	.149	.144	11	.358	.457	.245	.281
15	.036	.101	13	.242	.283	.196	.194
17	.029	.076	16	.137	.094	.164	.181
			18	.028	.057	.113	.155
			21	.001		.098	
			23	-.013		.060	
			26	-.034		.068	
			28	-.013		.055	
			31	-.022		.060	
			33	-.011		.062	
			36	-.013		.053	
			41	-.025		.066	
			46	.006		.057	
			51	.016		.062	
			56	.023		.057	

Table 5d. Velocity Measurements of Carbon Dioxide Jets at U_j = 25.4 m/s.

x/D_j	7		10			14	
r(mm)	w'/U_o	w'/U_o	r(mm)	U/U_o	u'/U_o	U/U_o	u'/U_o
0	.255	.255	0	1.000	.333	1.000	.372
1	-	-	1	.948	.326	.912	.387
2	.266	.257	2	.970	.332	.922	.358
3	-	-	3	.912	.323	.894	.371
4	.264	.266	4	.938	.333	.914	.373
5	-	-	5	.800	.328	.950	.373
6	.258	.253	6	.769	.335	.856	.383
7	-	-	7	.792	.315	.880	.375
8	.247	.245	8	.715	.330	.819	.375
10	.223	.217	10	.605	.317	.738	.359
12	.189	-	12	.427	.283	.561	.349
13	-	.151	15	.320	.248	.508	.368
14	.151	-	17	.294	.242	.442	.365
15	-	.138	20	.197	.205	.426	.305
17	.109	-	22	.103	.190	.303	.310
18	-	.102	25	.020	.148	.191	.298
19	.092	-	27	-.058	.109	.156	.255
20	-	.091	30	-.066	.102	.105	.235
22	.062	-	32	-.073	.095	.049	.210
23	-	.079	35	-.049	.085	-.140	.147
24	.069		40	-.068	.095	-.088	.179
27	.050		45	-.073	.102	-.109	.147
29	.047		50	-.061	.100	-.123	.126
32	.049		55	-.038	.105	-.133	.116
34	.040		60	-.036	.066	-.091	.116
37	.047						
42	.051						
47	.033						
52	.043						

Table 5e. Velocity Measurements of Carbon Dioxide Jets at U_j = 25.4 m/s.

x/D_j	20	
r(mm)	U/U_o	u'/U_o
0	1.000	.690
2	.992	.690
4	1.016	.698
6	1.008	.675
8	.992	.722
10	.992	.825
12	1.111	.675
15	.917	.746
20	.714	.730
25	.365	.603
30	.341	.611
35	.119	.530
40	-.087	.421
45	-.206	.444
50	-.262	.349
55	-.363	.317
60	-.381	.262

Table 6a. Velocity Measurements of Carbon Dioxide Jet at U_j = 54.0 m/s.

x/D_j	1.3		2					
r(mm)	U/U_o	u'/U_o	U/U_o	u'/U_o	w'/U_o	U/U_o	u'/U_o	w'/U_o
0	1.000	.318	1.000	.309	.141	1.000	.309	.141
1	.940	.331	.972	.307	.143	.953	.311	.138
2	.818	.320	.902	.316	–	.864	.304	–
3	.677	.306	.787	.307	.150	.729	.299	.143
4	.521	.286	.706	.304	–	.607	.283	–
5	.352	.237	.542	.285	.141	.449	.262	.136
6	.218	.183	.425	.257	–	.322	.220	–
7	.137	.135	.273	.204	.117	.240	.182	.113
8	.066	.091	.179	.164	–	.175	.150	–
9	–	–	–	–	.079	–	–	.085
10	.027	.043	.093	.091	–	.082	.078	.048
11	–	–	–	–	.057	–	–	.040
12	.005	.032	.039	.050	–	.019	.043	–
13	–	–	–	–	.054	–	–	.030
15	.008	.027	.013	.036	.036	.008	.035	.025
17	.002	.024	.003	.031	–			–
18	–	–	–	–	.041			.030
20	.005	.023	.003	.025	.040			
22	.002	.025	.007	.024	–			
23	–	–	–	–	.028			
25	.009	.019	.004	.027	.041			
27	.002	.023	.007	.022	–			
28	–	–	–	–	.032			
30	.007	.019	.004	.027	.031			
32	.003	.024	.005	.023	–			
33	–	–	–	–	.021			
35	.010	.018	.007	.024	.025			
38	–	–	–	–	.017			
40	.014	.012	.004	.028	–			
43	–	–	–	–	.014			
45	.005	.019	.006	.020	–			
48	–	–	–	–	.014			
50	.005	.016	.007	.021	–			

Table 6b. Velocity Measurements of Carbon Dioxide Jet at U_j = 54.0 m/s.

x/D_j	3		5				
r(mm)	U/U_o	u'/U_o	r(mm)	U/U_o	u'/U_o	U/U_o	u'/U_o
0	1.000	.320	0	1.000	.329	1.000	.329
.5	1.000	.320	1	.984	.310	.972	.322
1.5	.951	.320	2	.953	.329	.923	.334
2.5	.855	.322	3	.860	.329	.895	.329
3.5	.746	.310	4	.797	.323	.804	.329
4.5	.625	.298	5	.657	.315	.659	.312
5.5	.495	.276	6	.580	.305	.632	.310
6.5	.392	.249	7	.559	.280	.552	.287
7.5	.251	.191	8	.446	.273	.434	.266
8.5	.191	.170	10	.329	.224	.316	.229
9.5	.126	.126	12	.169	.173	.199	.183
10.5	.079	.120	15	.088	.135	.072	.112
13.5	.012	.056	17	-.022	.085	.047	.108
15.5	.014	.048	20	-.038	.066	-.010	.062
18.5	-.008	.037	22	-.018	.050		
20.5	-.008	.038	25	-.030	.041		
23.5	-.002	.033	27	-.026	.049		
25.5	-.003	.034	30	-.016	.038		
28.5	-.009	.033	32	-.019	.045		
30.5	-.002	.032	35	-.014	.043		
33.5	-.004	.032	40	-.001	.040		
38.5	.003	.028	45	.003	.043		
43.5	.002	.030	50	.007	.036		
48.5	-.001	.028	55	.011	.040		
53.5	.009	.024	60	.009	.040		

Table 6c. Velocity Measurements of Carbon Dioxide Jet at U_j = 54.0 m/s.

x/D_j	7					10	
r(mm)	U/U_o	u'/U_o	r(mm)	w'/U_o	w'/U_o	U/U_o	u'/U_o
0	1.000	.342	0	.211	.211	1.000	.373
1	.982	.337	1	-	-	1.000	.377
2	.998	.330	2	.213	.205	.974	.374
3	.871	.346	3	-	-	.943	.381
4	.869	.337	4	.215	.208	.909	.378
5	.820	.335	5	-	-	.922	.377
6	.700	.333	6	.209	.205	.857	.371
7	.627	.326	7	-	-	.831	.374
8	.586	.329	8	.201	.202	.746	.366
9	.577	.310	10	.193	.187	.649	.346
11	.421	.270	12	.182	.193	.560	.319
13	.270	.224	15	.144	.157	.418	.315
14	.207	.225	17	.108	.132	.327	.288
16	.141	.185	20	.096	.108	.219	.251
18	.103	.151	22	.095	.093	.106	.237
19	.045	.144	25	.072	.076	.046	.198
21	.041	.120	27	.076	.078	.053	.178
23	.013	.108	30	.064	.069	-.006	.156
24	-.026	.088	32	.059	.062	-.042	.138
26	-.039	.076	35	.053	.058	-.048	.121
29	-.037	.068	40	.042	.047	-.070	.095
31	-.038	.068	45	.044	.045	-.042	.104
34	-.049	.068	50	.045	044	-.064	.100
39	-.023	.066	55	.041	.044	-.079	.103
44	-.021	.059					
49	-.023	.064					
54	-.001	.061					
59	.001	.064					

Table 6d. Velocity Measurements of Carbon Dioxide Jet at U_j = 54.0 m/s.

x/D_j	14		20	
r(mm)	U/U_o	u'/U_o	U/U_o	u'/U_o
0	1.000	.484	1.000	.846
1	-	-	-	-
2	.996	.497	.881	.793
3	-	-	-	-
4	.968	.484	.881	.830
5	-	-	-	-
6	.941	.499	.952	.806
7	-	-	-	-
8	.945	.480	1.013	.802
10	.905	.495	.925	.868
12	.836	.503	.841	.877
15	.688	.465	.749	.855
17	.503	.448	.661	.903
20	.429	.453	.555	.881
22	.436	.413	.617	.863
25	.364	.404	.507	.859
27	.232	.379	.612	.841
30	.158	.341	.357	.859
32	.128	.316	.330	.780
35	.095	.295	.189	.793
40	-.069	.232	.026	.727
45	-.124	.221	.048	.634
50	-.141	.185	-.070	.573
55	-.152	.215	-.115	.515
60	-.154	.168	-.225	.467

Table 7a. Velocity Measurements of Air Jet at U_j = 25.4 m/s.

x/D_j	1.3			
r(mm)	U/U_o	u'/U_o	U/U_o	u'/U_o
0	1.000	.316	1.000	.316
1	.922	.302	.908	.285
2	.850	.301	.793	.281
3	.643	.285	.640	.278
4	.468	.251	.521	.251
5	.331	.203	.320	.204
6	.200	.148	.129	.144
7	.132	.115	.128	.097
8	.084	.071	.082	.065
10	.046	.027		
12	.027	.028		
15	.019	.021		
17	.014	.022		
20	.022	.021		
22	.011	.013		
25	.010	.015		
27	.012	.014		
30	.007	.014		
32	.009	.016		
35	.005	.018		
40	.003	.012		
45	-.002	.011		
50	-.002	.009		
55	-.007	.010		
60	-.007	.008		

Table 7b. Velocity Measurements of Air Jet at U_j = 25.4 m/s.

x/D_j	2						
r(mm)	U/U_o	u'/U_o	U/U_o	u'/U_o	r(mm)	w'/U_o	w'/U_o
0	1.000	.324	1.000	.324	0	.181	.181
1	.958	.322	.958	.312	.5	-	.180
2	.800	.318	.884	.318	1.5	.183	-
3	.697	.300	.744	.300	2.5	-	.175
4	.579	.283	.613	.277	3.5	.166	-
5	.426	.228	.435	.251	4.5	-	.161
6	.313	.191	.306	.219	5.5	.140	-
7	.248	.154	.198	.175	6.5	-	.128
8	.158	.118	.081	.121	7.5	.097	-
10	.067	.061	.066	.052	8.5	-	.082
12	.049	.038			9.5	.050	-
15	.042	.032			10.5	-	-
17	.028	.023			11.5	.030	.038
20	.045	.017			13.5	.025	.031
22	.028	.021			15.5	.015	
25	.017	.023			18.5	.014	
27	.017	.018			20.5	.013	
30	.010	.015					
32	.016	.018					
35	.010	.017					
40	.003	.016					
45	.004	.015					
50	-.002	.012					
55	-.009	.010					
60	-.009	.012					

Table 7c. Velocity Measurements of Air Jet at U_j = 25.4 m/s.

x/D_j	3		5				
r(mm)	U/U_o	u'/U_o	r(mm)	U/U_o	u'/U_o	U/U_o	u'/U_o
0	1.000	.362	0	1.000	.417	1.000	.417
1	.997	.362	1	1.063	.427	1.026	.404
2	.944	.345	2	1.031	.408	1.068	.404
3	.867	.332	3	.919	.408	1.035	.386
4	.756	.313	4	.888	.404	.882	.357
5	.548	.296	5	.737	.355	.754	.364
6	.418	.259	6	.608	.353	.706	.340
7	.282	.181	7	.522	.307	-	-
8	.245	.170	8	.443	.256	.496	.314
10	.090	.107	9	.318	.228	.250	.232
12	.035	.068	10	.254	.191	.188	.200
15	.055	.032	12	.211	.148		
17	.022	.030	14	.131	.110		
20	.044	.030	17	.074	.082		
22	.036	.027	19	.042	.074		
25	.020	.027	22	.055	.061		
27	.024	.029	24	.037	.051		
30	.033	.024	27	.040	.051		
32	-.014	.036	29	.035	.044		
35	.010	.024	32	.028	.043		
40	-.001	.023	34	-.037	.055		
45	-.004	.019	37	-.018	.055		
			42	-.035	.039		
			47	-.018	.034		
			52	-.006	.021		
			57	-.018	.026		
			62	-.017	.034		

Table 7d. Velocity Measurements of Air Jet at U_j = 25.4 m/s.

x/D_j	7						
r(mm)	U/U_o	u'/U_o	U/U_o	u'/U_o	r(mm)	w'/U_o	w'/U_o
0	1.000	.488	1.000	.488	0	.424	.424
1	.997	.488	1.003	.491	.5	-	.424
2	-	-	-	-	1.5	.418	-
3	1.026	.491	.959	.471	2.5	-	.418
4	-	-	-	-	3.5	.426	-
5	.846	.442	.840	.442	4.5	-	.418
6	-	-	-	-	5.5	.379	-
7	.674	.395	.689	.395	6.5	-	.396
8	-	-	-	-	7.5	.390	-
9	.488	.320	.427	.328	8.5	-	.376
10	.422	.277	-	-	9.5	.334	-
11	.416	.272	-	-	10.5	-	.315
12	-	-	.317	.299	11.5	.276	-
13	.277	.236			13.5	.241	.284
15	.253	.194			15.5	-	.212
17	-	-			16.5	.231	-
18	.209	.177			18.5	.176	.206
20	.134	.150			20.5	-	.123
23	.128	.117			21.5	.111	-
25	.073	.101			23.5	.103	.111
28	.073	.084			25.5	-	.100
30	.033	.072			26.5	.103	
33	-.009	.066			28.5	.089	
35	.035	.074			31.5	.084	
38	.020	.064			33.5	.078	
43	.028	.047			36.5	.081	
48	-.025	.055			41.5	.064	
53	.017	.040			46.5	.072	
58	-.012	.044			51.5	.064	
62	-.020	.044			56.5	.067	

Table 7e. Velocity Measurements of Air Jet at U_j = 25.4 m/s.

x/D_j	10	
r(mm)	U/U_o	u'/U_o
0	1.000	.838
1	1.192	.846
2	1.269	.954
4	1.554	.931
5	1.408	1.038
6	1.508	1.008
8	1.385	1.008
10	1.469	.985
12	1.054	.885
15	1.085	.892
17	.608	.715
20	.592	.700
22	.146	.562
25	.108	.585
27	.128	.508
30	.046	.510
32	-.069	.408
35	-.230	.300
40	-.246	.300

Table 8a. Velocity Measurements of Air Jet at U_j = 66.8 m/s.

x/D_j	1		2		3		
r(mm)	U/U_o	u'/U_o	w'/U_o	w'/U_o	r(mm)	U/U_o	u'/U_o
0	1.000	.313	.171	.171	0	1.000	.344
1	.911	.310	.171	.171	1	.920	.319
2	.812	.301	-	-	2	.812	.300
3	.709	.267	.172	.172	3	.707	.274
4	.628	.250	-	-	4	.573	.271
5	.444	.218	.161	.162	6	.309	.194
6	.291	.178	-	-	7	.248	.171
7	.198	.132	.137	.148	9	.119	.108
8	-	-	-	-	12	.063	.047
9	.081	.055	.110	.098	14	.049	.035
10	.049	.041	-	-	17	.036	.034
11	-	-	.082	-	19	.027	.028
12	.041	.026	-	.058	22	.020	.026
13	-	-	.062	-	24	.045	.029
14	-	-	-	.059	27	.008	.027
15	.028	.022	.049	-	29	.003	.030
17	.026	.019	-	.041	32	-.003	.024
18	-	-	.046	-	34	-.002	.024
19	-	-	-	.044	37	-.003	.022
20	.016	.017	.038	-	39	-.005	.021
22	.010	.016	-	.040	44	-.006	.020
23	-	-	.045	-	49	-.009	.020
25	.014	.017	.042				
27	.013	.016	-				
28	-	-	.045				
30	.013	.016					
32	.013	.013					
35	.012	.012					
37	.011	.012					
40	.010	.012					
52	.012	.015					

Table 8b. Velocity Measurements of Air Jet at U_j = 66.8 m/s.

x/D_j	5		7			
r(mm)	U/U_o	u'/U_o	U/U_o	u'/U_o	w'/U_o	w'/U_o
0	1.000	.333	1.000	.367	.271	.271
1	.961	.329	–	–	–	–
2	.876	.311	.963	.343	.272	.274
3	–	–	.840	.336	–	–
4	.715	.283	–	–	.272	.274
5	.673	.285	.760	.315	–	–
6	–	–	–	–	.278	.269
7	.432	.238	–	–	–	–
8	–	–	.542	.280	.270	.267
10	.216	.154	.434	.239	.253	.255
12	.155	.122	–	–	.232	.232
13	–	–	.284	.221	–	–
15	.091	.085	.224	.192	.199	.204
17	.065	.063	–	–	.184	.168
18	–	–	.094	.147	–	–
20	.030	.059	.080	.134	.148	.138
22	.016	.062	–	–	.144	.125
23	–	–	.024	.107	–	–
25	.016	.043	.002	.096	.115	.111
27	-.008	.049	–	–	.104	.106
28	–	–	-.017	.082	–	–
30	-.018	.041	-.030	.081	.084	.094
32	-.015	.042	–	–	.081	.087
33	–	–	-.030	.074	–	–
35	-.019	.043	-.038	.073	.077	.077
37	-.023	.043	–	–	–	–
40	–	–	-.051	.062	.066	.063
42	-.016	.039	–	–	–	–
45	–	–	-.060	.062	.060	.060
47	-.023	.045	–	–	–	–
50	–	–	–	–	–	.061

Table 8c. Velocity Measurements of Air Jet at U_j = 66.8 m/s.

x/D_j	10				14			
r(mm)	U/U_o	u'/U_o	U/U_o	u'/U_o	U/U_o	u'/U_o	U/U_o	u'/U_o
0	1.000	.637	1.000	.637	1.000	1.387	1.000	1.387
2	.986	.623	.952	.613	.852	1.437	.929	1.415
4	.760	.609	.810	.567	.817	1.324	.796	1.373
6	.804	.551	.818	.591	.782	1.359	.760	1.282
8	.710	.505	.665	.565	.697	1.282	.852	1.366
10	.653	.539	.581	.563	.852	1.345	1.030	1.437
12	.553	.461	.503	.529	.676	1.317	.528	1.239
14	.379	.399	.463	.499	.507	1.239	.493	1.246
16	.311	.369	.331	.429	.535	1.120	.458	1.120
18	.259	.345	.206	.417	.317	1.049	.359	1.155
20	.291	.317	.140	.385	.507	1.049		
22	.225	.305	.068	.351	.450	1.070		
24	.148	.261			.577	1.211		
26	.158	.259			.310	1.098		
28	.138	.317			.401	1.155		
30	.078	.251			.296	1.106		
32	.068	.226			.260	.873		
34	.074	.222			.218	.944		
36					.197	.908		
38					.092	.810		
40					.141	.789		

Table 9a. Velocity Measurements of Air Jet at U_j = 152.8 m/s.

x/D_j	1.25		2			
r(mm)	U/U_o	u'/U_o	U/U_o	u'/U_o	U/U_o	u'/U_o
0	1.000	.213	1.000	.225	1.000	.225
1	.950	.222	.944	.239	.975	.229
2	.865	.250	.894	.263	.927	.242
3	.726	.273	.841	.274	.856	.260
4	.642	.291	.745	.295	.770	.275
5	.461	.291	.609	.306	.616	.290
6	.280	.226	.409	.288	.487	.290
7	.205	.180	.278	.236	-	-
8	.096	.119	.194	.184	.223	.213
9	.039	.079	.111	.136	-	-
10	.023	.055	.069	.092	.065	.090
12	.014	.047	.020	.059	-	-
13	-	-	-	-	.022	.052
14	.014	.047	.022	.046		
17	0	.041	.001	.041		
19	.005	.041	-.001	.044		
22	.019	.030	-.003	.047		
24	.005	.034	-.002	.041		
27	.013	.033	.009	.037		
29	.016	.034	.005	.039		
32	.014	.033	.007	.035		
34	.006	.032	.002	.040		
37	.008	.031	.005	.037		
42	.004	.029	.006	.037		
47	.001	.033	.003	.033		
52	.007	.025	.005	.031		
57	.006	.027	.008	.028		
62	.0005	.027	.007	.034		

Table 9b. Velocity Measurements of Air Jet at U_j = 152.8 m/s.

x/D_j	2		3			5		
r(mm)	w'/U_o	w'/U_o	r(mm)	U/U_o	u'/U_o	r(mm)	U/U_o	u'/U_o
0	.237	.237	0	1.000	.240	0	1.000	.281
1	.237	.237	1	1.009	.238	2	.995	.284
3	.242	.240	2	.982	.255	4	.918	.293
5	.226	.215	3	.946	.260	5	.835	.297
7	.194	.176	4	.902	.250	6	.685	.272
9	.134	.133	5	.780	.253	7	.665	.264
11	.087	-	6	.719	.250	8	.560	.264
12	-	.066	7	.642	.250	9	.518	.253
13	.071	-	8	.461	.250	10	.452	.235
14	-	.068	9	.369	.205	11	.361	.210
15	.064	-	10	.251	.162	12	.287	.185
17	-	.056	12	.142	.095	14	.182	.145
18	.062	-	14	.041	.069	16	.135	.105
19	-	.047	17	.020	.049	19	.075	.081
20	.063	-	19	-.003	.045	21	.069	.066
22	-	.053	22	0	.041	24	.046	.059
23	.059	-	24	-.003	.041	26	.012	.057
25	.050	-	27	-.010	.035	29	.004	.054
28	.050	-	29	-.017	.038	31	-.005	.047
			32	-.023	.038	34	-.006	.045
			34	-.021	.037	36	-.014	.045
			37	-.023	.035	39	-.020	.042
			42	-.026	.037	44	-.021	.040
			47	-.010	.033	49	-.022	.037
			52	-.010	.033	54	-.021	.033
			57	-.010	.036	59	-.029	.032
			62	-.002	.034	62	-.028	.034

Table 9c. Velocity Measurements of Air Jet at U_j = 152.8 m/s.

x/D_j	7				
r(mm)	U/U_o	u'/U_o	r(mm)	w'/U_o	w'/U_o
0	1.000	.328	0	.209	.209
1	.996	.311	1	.193	.209
2	.970	.328	3	.193	.209
3	.930	.338	5	.195	.206
4	.874	.335	7	.199	.206
5	.878	.348	9	.189	.190
6	.793	.377	11	.179	.182
7	.693	.337	13	-	.177
8	.700	.345	14	.167	-
9	.681	.337	16	.152	.143
10	.495	.334	18	-	.127
11	.384	.292	19	.128	-
12	.396	.309	21	.108	.104
13	.361	.298	23	-	.090
15	.194	.215	24	.101	-
17	.147	.199	26	.083	.091
20	.067	.143	28	-	.084
22	.031	.113	29	.081	-
25	-.003	.087	31	.088	.091
27	-.008	.078	33	-	.076
30	-.033	.061	34	.068	-
32	-.035	.060	36	-	.071
35	-.033	.058	39	.061	-
37	-.034	.054	41	-	.062
40	-.038	.052	44	.061	-
45	-.039	.059	46	-	.052
50	-.041	.057	49	.051	-
55	-.032	.054			
60	-.037	.056			

Table 9d. Velocity Measurements of Air Jet at U_j = 152.8 m/s.

x/D_j	10				14		
r(mm)	U/U_o	u'/U_o	U/U_o	u'/U_o	r(mm)	U/U_o	u'/U_o
0	1.000	.405	1.000	.405	0	1.000	.534
2	.942	.419	-	-	2	.955	.564
3	-	-	.936	.417	3	1.052	.583
4	.959	.402	-	-	4	1.076	.578
5	-	-	.850	.384	5	.900	.549
6	.820	.396	-	-	6	1.019	.579
8	.791	.397	.800	.401	8	.965	.561
10	.616	.356	.721	.364	10	.836	.545
12	.599	.349	-	-	12	.838	.523
13	.529	.335	.599	.326	13	.755	.524
14	.452	.316	-	-	15	.768	.498
15	.386	.300	.494	.306	18	.633	.464
16	.395	.304	-	-	20	.622	.473
17	.369	.294	-	-	23	.491	.422
18	.297	.271	.390	.263	28	.377	.357
19	.256	.244	-	-	33	.278	.321
20	.276	.257	.287	.222	38	.055	.252
22	.181	.217	-	-	43	-.020	.209
23	-	-	.215	.200			
24	.126	.184					
27	.081	.158					
29	.022	.120					
32	.004	.103					
34	-.001	.118					
37	-.034	.082					
39	-.051	.072					
42	-.059	.070					
44	-.048	.072					
47	-.060	.068					
52	-.062	.063					
57	-.059	.061					
62	-.070	.059					

Table 9e. Velocity Measurements of Air Jet at U_j = 152.8 m/s.

x/D_j	20		40		
r(mm)	U/U_o	u'/U_o	r(mm)	U/U_o	u'/U_o
0	1.000	.750	0	1.000	2.097
2	.926	.725	1	.355	1.495
4	.994	.722	3	.183	1.828
6	1.014	.730	4	.538	2.043
7	.873	.762	5	.355	1.903
8	.865	.686	6	.731	2.054
9	.876	.739	7	.280	1.624
10	1.007	.787	8	.871	2.011
11	.924	.755	10	.538	2.290
12	.826	.737	12	.538	1.957
14	.847	.728	15	.398	2.054
16	.839	.769	17	1.065	2.054
17	.775	.700	20	1.247	2.355
18	.884	.762	22	.419	2.032
19	.775	.699	25	.882	1.860
20	.690	.711	27	.237	1.989
22	.692	.652	30	.559	2.032
23	.725	.731	32	1.484	2.333
24	.624	.638	35	.656	2.269
25	.718	.711	40	.548	2.505
27	.618	.615	45	.043	2.484
28	.638	.702	50	.882	2.753
30	.592	.679	55	.462	2.699
32	.507	.553	60	.226	2.409
35	.500	.622			
37	.362	.520			
38	.392	.584			
42	.266	.439			
47	.244	.419			
52	.208	.366			
58	.084	.348			

Table 10a. Velocity Measurements of Helium/Air Jet at U_j = 16.8 m/s.

x/D_j	2			
r(mm)	U/U_o	u'/U_o	w'/U_o	w'/U_o
0	1.000	.417	.239	.239
.5	1.000	.417	-	.241
1.5	1.007	.414	.230	-
2.5	.985	.417	-	.238
3.5	.904	.399	.224	-
4.5	.844	.371	.218	.220
5.5	.763	.323	.190	-
6.5	.522	.292	.170	.187
7.5	.022	.059	.154	-
8.5	.002	.040	.132	.138
9.5	-.011	.042	.097	.082
10.5			.072	-
11.5			.045	.048
12.5			-	-
13.5			.033	.028
15.5			.031	
18.5			.026	
20.5			.019	
23.5			.022	

Table 10b. Velocity Measurements of Helium/Air Jet at U_j = 16.8 m/s.

x/D_j	3		5		7	
r(mm)	U/U_o	u'/U_o	U/U_o	u'/U_o	U/U_o	u'/U_o
0	1.000	.331	1.000	.422	1.000	.588
.5	.975	.326	1.000	.422	1.000	.588
1.5	1.000	.331	1.123	.431	.987	.618
2.5	.732	.306	1.123	.434	.865	.585
3.5	.683	.284	.855	.428	.884	.601
4.5	.553	.261	1.003	.443	.858	.601
5.5	.490	.250	.711	.391	1.348	.628
6.5	.391	.226	.492	.302	.671	.572
7.5	.333	.228	.400	.291	.665	.532
9.5	.284	.196	.243	.243	.582	.517
10.5	-.076	.148	.262	.299	.608	.495
12.5	-.038	.102	.128	.240	.405	.470
15.5	-.021	.010	.019	.167	.313	.387
17.5	-.014	.012	-.062	.111	.071	.303
20.5	-.018	.014				
22.5	-.019	.023				
25.5	-.016	.026				
27.5	-.021	.017				
30.5	-.035	.024				
32.5	-.008	.017				
35.5	-.007	.018				
37.5	-.009	.021				
40.5	-.013	.017				
42.5	-.021	.015				
47.5	-.017	.006				
52.5	-.012	.006				
55.5	-.006	.007				
57.5	-.008	.006				
59.5	-.003	.005				

Table 10c. Velocity Measurements of Helium/Air Jet at U_j = 16.8 m/s.

x/D_j	7		10		
r(mm)	w'/U_o	w'/U_o	r(mm)	U/U_o	u'/U_o
0	.465	.465	0	1.000	.639
1	-	-	.5	1.000	.585
2	.465	.452	1.5	1.000	.639
3	-	-	2.5	.955	.574
4	.465	.455	3.5	.679	.577
5	-	-	4.5	.793	.610
6	.471	.426	5.5	.635	.627
7	.452	-	6.5	.668	.607
8	.439	.406	7.5	.434	.574
10	.432	.432	9.5	.430	.574
12	.406	.355	10.5	.410	.634
15	.355	.297	12.5	.359	.515
17	.323	.265	15.5	.336	.517
20	.219	.265	17.5	.061	.436
22	.181	.161			
25	.168	.155			
27	.116	.110			
30	.116	.110			

Table 11a. Velocity Measurements of Helium/Air Jet at U_j = 36.5 m/s.

x/D_j	2				
r(mm)	U/U_o	u'/U_o	r(mm)	w'/U_o	w'/U_o
0	1.000	.300	0	.166	.166
.5	.951	.315	2	.165	.163
1.5	1.000	.300	4	.162	.164
2.5	.955	.310	5	.156	-
3.5	.821	.311	6	.145	.150
4.5	.646	.291	7	.127	-
5.5	.474	.284	8	.104	.122
6.5	.359	.229	9	.091	-
7.5	.268	.203	10	.065	-
9.5	.031	.055	11	.062	.057
10.5	.020	.039	12	.040	-
12.5	-.002	.029	13	-	.043
15.5	-.002	.023	14	.026	-
17.5	-.003	.015	16	.021	.026
			19	.017	
			21	.018	
			24	.017	

Table 11b. Velocity Measurements of Helium/Air Jet at U_j = 36.5 m/s.

x/D_j	3		5		7	
r(mm)	U/U_o	u'/U_o	U/U_o	u'/U_o	U/U_o	u'/U_o
0	1.000	.339	1.000	.325	1.000	.468
.5	1.000	.339	.997	.325	1.000	.468
1.5	1.002	.334	.920	.336	.947	.474
2.5	.958	.329	.815	.351	.991	.474
3.5	.893	.334	.732	.325	.965	.477
4.5	.754	.341	.646	.321	.962	.480
5.5	.707	.310	.545	.298	1.053	.480
6.5	.540	.301	.545	.292	.731	.456
7.5	.415	.269	.407	.264	.708	.450
9.5	.225	.209	-	-	-	-
10.5	.129	.174	.148	.179	.494	.412
12.5	.016	.111	.083	.154	.453	.386
15.5	-.019	.061	-.011	.102	.206	.304
17.5	-.037	.027	-.054	.070	.135	.227
20.5	-.034	.025			-.114	.149
22.5	-.031	.024			-.085	.143
27.5	-.024	.024				
32.5	-.031	.023				
37.5	-.017	.024				
42.5	-.010	.034				
47.5	-.005	.026				
52.5	-.003	.026				

Table 11c. Velocity Measurements of Helium/Air Jet at U_j = 36.5 m/s.

x/D_j	7		10		
r(mm)	w'/U_o	w'/U_o	r(mm)	U/U_o	u'/U_o
0	.360	.360	0	1.000	.566
2	.354	.351	.5	1.000	.570
4	.322	.339	1.5	.934	.526
6	.325	.330	2.5	.798	.513
8	.310	.330	3.5	.772	.504
9	.310	-	4.5	.763	.509
10	.301	.289	5.5	.768	.513
12	.265	-	6.5	.675	.500
13	-	.272	7.5	.596	.509
14	.249	-	9.5	.710	.500
15	-	.237	10.5	.710	.544
17	.199	-	12.5	.531	.478
18	-	.187	15.5	.399	.478
19	.167	-	17.5	.254	.474
20	-	.143	20.5	.070	.381
22	.135	-	22.5	.005	.329
23	-	.105			
24	.091	-			
25	-	.076			
27	.070	-			
28	-	.079			
29	.076				
32	.064				

Table 12. Values of K and Jet Half-width for Different x/D_j Locations.

$\frac{x}{D_j}$	Airjet at U_j = 152.8 m/s (dashed curves)		All other jets (solid curves)	
	K	$r_{1/2}$(mm)	K	$r_{1/2}$(mm)
1.25(1.3)	4.17	4.45	4.17	4.45
2	6.28	5.80	9.37	4.75
3	9.00	7.27	16.23	5.41
5	14.72	9.48	32.81	6.34
7	23.93	10.40	29.81	9.32
10	26.16	14.22	38.94	11.65
14	20.27	22.60	51.16	14.23
20	19.40	33.00	36.68	24.00

1. Report No.	2. Government Accession No.	3. Recipient's Catalog No.
NASA CR-174829		

4. Title and Subtitle	5. Report Date
Behavior of Turbulent Gas Jets in an Axisymmetric Confinement	January 1985
	6. Performing Organization Code

7. Author(s)	8. Performing Organization Report No.
Ronald M. C. So and Saad A. Ahmed	CR-R-84041
	10. Work Unit No.

9. Performing Organization Name and Address	11. Contract or Grant No.
Arizona State University Mechanical and Aerospace Engineering Tempe, Arizona 85287	NAG 3-260
	13. Type of Report and Period Covered
12. Sponsoring Agency Name and Address	Contractor Report
National Aeronautics and Space Administration Washington, D.C. 20546	14. Sponsoring Agency Code
	505-31-04

15. Supplementary Notes

Final report. Project Manager, Russell W. Claus, Internal Fluid Mechanics Division, NASA Lewis Research Center, Cleveland, Ohio 44135.

16. Abstract

The understanding of the mixing of confined turbulent jets of different densities with air is of great importance to many industrial applications, such as gas turbine and ramjet combustors. Although there have been numerous studies on the characteristics of free gas jets, little is known of the behavior of gas jets in a confinement. The present investigation addresses this question directly and reports on the fluid dynamics of confined turbulent gas jets. The jet, with a diameter of 8.73 mm, is aligned concentrically in a tube of 125 mm diameter, thus giving a confinement ratio of ~205. The arrangement forms part of the test section of an open-jet wind tunnel. Experiments are carried out with carbon dioxide, air and helium/air jets at different jet velocities. Mean velocity and turbulence measurements are made with a one-color, one-component laser droppler velocimeter operating in the forward scatter mode. Measurements show that the jets are highly dissipative. Consequently, equilibrium jet characteristics similar to those found in free air jets are observed in the first two diameters downstream of the jet. These results are independent of the fluid densities and velocities. Decay of the jet, on the other hand, is a function of both the jet fluid density and momentum. In all the cases studied, the jet is found to be completely dissipated in ~30 jet diameters, thus giving rise to a uniform flow with a very high but constant turbulence field across the confinement.

17. Key Words (Suggested by Author(s))	18. Distribution Statement
Turbulent jets; Confined jets; Inhomogeneous jets; Turbulent mixing; Confined flows	Unclassified - unlimited STAR Category 07

19. Security Classif. (of this report)	20. Security Classif. (of this page)	21. No. of pages	22. Price*
Unclassified	Unclassified	92	A05

*For sale by the National Technical Information Service, Springfield, Virginia 22161